MOLECULAR AND CELLULAR BIOLOGY, Apr. 2010, p. 1729–1745 Vol. 30, No. 7
0270-7306/10/$12.00 doi:10.1128/MCB.00952-09
Copyright © 2010, American Society for Microbiology. All Rights Reserved.

Regulation of RB Transcription *In Vivo* by RB Family Members▽‡

Deborah L. Burkhart,[1,2]† Lynn K. Ngai,[1] Caitlin M. Roake,[1] Patrick Viatour,[1] Chellappagounder Thangavel,[3] Victoria M. Ho,[1]# Erik S. Knudsen,[3] and Julien Sage[1,2]*

Departments of Pediatrics and Genetics[1] and Cancer Biology Program,[2] Stanford Medical School, Stanford, California 94305, and Kimmel Cancer Center, Thomas Jefferson University, Philadelphia, Pennsylvania 19107[3]

Received 20 July 2009/Returned for modification 22 August 2009/Accepted 13 January 2010

In cancer cells, the retinoblastoma tumor suppressor RB is directly inactivated by mutation in the *RB* gene or functionally inhibited by abnormal activation of cyclin-dependent kinase activity. While variations in *RB* levels may also provide an important means of controlling RB function in both normal and cancer cells, little is known about the mechanisms regulating *RB* transcription. Here we show that members of the RB and E2F families bind directly to the *RB* promoter. To investigate how the RB/E2F pathway may regulate *Rb* transcription, we generated reporter mice carrying an *eGFP* transgene inserted into a bacterial artificial chromosome containing most of the *Rb* gene. Expression of eGFP largely parallels that of *Rb* in transgenic embryos and adult mice. Using these reporter mice and mutant alleles for *Rb*, *p107*, and *p130*, we found that RB family members modulate *Rb* transcription in specific cell populations *in vivo* and in culture. Interestingly, while *Rb* is a target of the RB/E2F pathway in mouse and human cells, *Rb* expression does not strictly correlate with the cell cycle status of these cells. These experiments identify novel regulatory feedback mechanisms within the RB pathway in mammalian cells.

The *RB* tumor suppressor gene was first identified through its direct mutation or deletion in human retinoblastoma. The RB protein is thought to function largely as a transcriptional cofactor that can repress or potentiate the functions of numerous transcription factors, affecting the expression of a broad number of target genes. Since its initial discovery, RB function has been demonstrated to be inactivated in virtually all human cancers through a variety of mechanisms. In particular, in addition to direct mutation events in the *RB* gene, the RB protein is often functionally inactivated by phosphorylation in tumor cells with constitutive activation of cyclin/Cdk complexes (44, 55). *RB* inactivation through reduced transcription may also participate in the development of cancer (4, 41); surprisingly, however, little is known about the mechanisms regulating *RB* transcription in normal and tumor cells.

Interestingly, the *RB* promoter contains a conserved binding site for the E2F transcription factors, some of which are direct partners of RB and key downstream mediators of RB (9). Increasing evidence suggests that this site may contribute to the regulation of *RB* transcription. For instance, overexpression of E2F1 can activate *RB* transcription, which may contribute to the variations in *RB* mRNA levels during cell cycle progression that are observed in some contexts (30, 43) but not in others (5, 13, 20). In addition, methylation of the E2F site in the *RB* promoter is sufficient to recruit repressor complexes to inhibit *RB* transcription (15). Accordingly, reporter assays show that mutation of the E2F site in the *RB* promoter leads to an absence of *RB* repression (33). Furthermore, mutation of the E2F (and Sp1) sites in the mouse *Rb* promoter in transgenic mice has revealed the importance of these sites for *Rb* expression *in vivo* (1).

Together, these data suggest that upstream members of the RB pathway, including RB itself, may regulate *RB* transcription via their action on the E2F family. Indeed, analysis of the transcription of mutant *RB* alleles suggests that RB may regulate its own expression in the cells of retinoblastoma patients (17). In addition, in both bladder and melanoma tumor cells that functionally inactivate RB through phosphorylation, increased levels of RB protein have been observed (3, 38), further suggesting that activity of the RB protein may regulate the expression of *RB*. Overexpression of RB is also capable of repressing an *RB* reporter construct in P19 cells (22). However, the E2F binding site is not necessary for RB-mediated autoregulation in all contexts (19), and RB may positively regulate its own promoter through an ATF binding site (35) or an independent element (18). Furthermore, mutation of the E2F binding site in the *RB* promoter results in increased reporter expression, even in *RB*-deficient cells (33), suggesting that another factor may repress *RB* through E2F. In mammalian cells, the p107 and p130 proteins are structurally and functionally related to RB and interact with E2F transcription factors (10), raising the possibility that these two RB family members may regulate the *RB* promoter. In support of this idea, loss of *p107* in mouse embryos results in increased *Rb* levels, although it is unclear if this represents a direct effect of p107 on the *Rb* promoter (16, 28).

Here we sought to clarify the regulation of *Rb* expression by the three pocket proteins, RB, p107, and p130, in cells in culture and in various organs and tissues in mice. Using chromatin immunoprecipitation and a novel *Rb* transgenic reporter

* Corresponding author. Mailing address: Department of Pediatrics, 269 Campus Drive, CCSR1215, Stanford, CA 94305. Phone: (650) 724-9246. Fax: (650) 736-0195. E-mail: julien.sage@stanford.edu.

† Present address: Department of Pathology, UCSF, San Francisco, CA 94143.

Present address: Interdepartmental Program in Neuroscience and Medical Scientist Training Program, UCLA, Los Angeles, CA 90095.

▽ Published ahead of print on 25 January 2010.

‡ The authors have paid a fee to allow immediate free access to this article.

Downloaded from https://journals.asm.org/journal/mcb on 24 February 2022 by 2a01:4f9:3b:1ae9::

line, we showed that expression of the mouse *Rb* gene is controlled by its own gene product and p107 and p130 *in vivo*. Interestingly, however, *Rb* expression does not always increase during cell cycle progression, indicating that *Rb* is not a canonical E2F target gene. These experiments provide novel insights into the mechanisms regulating RB levels in cells and identify an additional level of complexity in the RB pathway in mammalian cells.

MATERIALS AND METHODS

Abbreviations. Abbreviations used in this study are as follows: RB, mouse and human retinoblastoma protein; *RB*, human gene; *Rb*, mouse gene; MEFs, mouse embryonic fibroblasts; ChIP, chromatin immunoprecipitation; FACS, fluorescence-activated cell sorting (or sorter); BAC, bacterial artificial chromosome; eGFP, enhanced green fluorescent protein; RT-qPCR, quantitative reverse transcription-PCR; TKO, triple knockout; ATF, activating transcription factor; DMEM, Dulbecco's modified Eagle's medium; shRNA, short hairpin RNA; PBS, phosphate-buffered saline; BSA, bovine serum albumin; FITC, fluorescein isothiocyanate; PBST, PBS plus 0.1% Tween; FAM, 6-carboxyfluorescein; BHQ, black hole quencher; gDNA, genomic DNA; PI, propidium iodide; E15.5, 15.5 days postfertilization; Ad-Cre, adenovirus expressing the Cre recombinase; UTR, untranscribed region; DMSO, dimethyl sulfoxide.

Cell culture. MEFs and NIH 3T3, MCF7, Saos2, and T98G cells were cultured in media supplemented with 10% serum, penicillin-streptomycin, and L-glutamine. MEFs were used between passages 3 and 5 for knockout experiments. To delete *Rb*, 3×10^5 $Rb^{lox/lox}$; *Rb-eGFP* MEFs were infected with Adeno-empty (empty adenovirus, no Cre expressed; also referred to as control adenovirus) or Adeno-Cre (University of Iowa gene transfer core) as they were plated in DMEM supplemented with 10% serum. Cells were allowed to grow for 3 days before being replated for an asynchronous or quiescence experiment. For quiescence experiments, cells were plated and then cultured in 0.1% serum for 3 days. For MEF and T98G synchronization experiments, cells were plated at subconfluence in 0.1% serum and kept in a low concentration of serum for 3 days. Synchronized cell cycle reentry for both cell types was induced through the addition of medium containing 20% serum. $Rb^{lox/lox}$; $p130^{lox/lox}$; $p107^{-/-}$; $Rosa26^{CreERT2}$; *Rb-eGFP* BAC MEFs were generated from embryos 13.5 days after fertilization and cultured as above. Samples were collected 4 days after being infected with Adeno-empty or Adeno-Cre in 10% serum. Immortal MEFs were generated through retroviral infection with a vector that expresses shRNA molecules directed against $p19^{ARF}$ (39). For Hoechst-based cell sorting, subconfluent, immortalized MEFs were trypsinized and resuspended in DMEM plus 10% serum at 10×10^6 cells/ml. Hoechst 33342 stain was added at 30 μg/ml, and the cells were incubated at 37°C for 1 h in the dark. Cells were spun and resuspended in 1 ml of DMEM with fresh Hoechst, filtered through a 40-μm cell strainer, and then sorted by FACS.

MCF7 cells were treated with 500 nM PD 033291 (a chemical inhibitor of the CDK4 kinase; Pfizer) for 72 h. Saos2 cells were transfected with plasmids expressing GFP-RB, GFP-p107, GFP-p130, or GFP individually, as described previously (47). Cells were processed for ChIP assay 48 h posttransfection.

Chromatin immunoprecipitation. Chromatin immunoprecipitation was performed as described previously (2, 56). Briefly, NIH3T3 fibroblasts and T98Gs were trypsinized, washed once with PBS, and fixed in DMEM with 1% formaldehyde for 15 min at room temperature. Fixation was quenched by the addition of glycine to a final concentration of 0.125 M for 5 min at room temperature. Fixed cells were washed in ice-cold PBS, pelleted, and frozen at −80°C. Cells were lysed, and nuclear extracts were sonicated through 12 30-s pulses on a Vircell sonicator at 4°C. Affi-Prep protein A support (Bio-Rad) was blocked overnight with salmon sperm DNA and BSA. Immunoprecipitations were performed overnight at 4°C. Antibodies used for immunoprecipitations were as follows: p107 (sc-318X), p130 (sc-317X), E2F1 (sc-193X), E2F3 (sc-878X), E2F4 (sc-1082X), ATF-2 (sc-187X), Sp1 (sc-59X), and p16 (sc-467). *Rb* promoter binding was assessed through quantitative PCR using SYBR GreenER master mix (Invitrogen). Mouse *Rb* primers, described previously (14), were as follows: forward primer, 5′-CGCCGCGGGCGGAAGTG-3′; reverse primer, 5′-CTCA CCCGACTCCCGTTAC-3′; *actin* forward primer, 5′-GCTTCTTTGCAGCTC CTTCGTTG-3′; and *actin* reverse primer, 5′-TTTGCACATGCCGGAGCCGT TGT-3′. In the T98G cells, the mouse *Rb* primers were used to amplify the human promoter, due to sufficient conservation. *CDC6* primers used were as follows: forward, 5′-TCTTGACACTTCCAGTCGAAGGA-3′, and reverse, 5′-TAGAGTCGCTGTGAGGCCACGACCACTG-3′. The control primers were forward, 5′-ATGGTTGCCACTGGGGATCT-3′, and reverse, 5′-TGCCAAAG CCTAGGGGAAGA-3′.

Transient ChIP analysis in Saos2 cells was described recently (47). In brief, purified DNA from immunoprecipitations using the GFP and Dbf4 antibodies were PCR amplified using human *RB* promoter primers forward, 5′-GGCGGA AGTGACGTTTTC-3′, and reverse, 5′-CCGACTCCCGTTACAAAAAT-3′, and human *albumin* promoter primers forward, 5′-CAGGGATGGAAAGAAT CCTATGCC-3′, and reverse, 5′-CCATGTTCCCATTCCTGCTGT-3′. Anti-Dbf4 and human *albumin* promoters served as negative controls. The PCR-amplified products were subjected to 2% agarose gel electrophoresis, stained with ethidium bromide, visualized through UV transillumination, and documented using the Eagle Eye system.

Generation of *Rb-eGFP* BAC transgenic mice and other mouse strains. Recombineering was used to generate the *Rb-eGFP* BAC, as described previously (8). Briefly, BAC clone RP24-370G12, ordered from BACPAC (http://bacpac.chori.org/), was transformed into the recombineering strain EL250. The heat-inducible recombinase present in this strain enabled the insertion of an *eGFP* cDNA, including two polyadenylation signals at the translation start site of *Rb* by homologous recombination. The *Rb-eGFP* BAC was purified, using a Marligen maxiprep kit. BAC DNA was injected into F1 hybrid B6D2F1/J (100006; The Jackson Laboratory)-fertilized oocytes at the Stanford Transgenic Research Facility. This injection resulted in two germ line founders. Genotyping of *Rb-eGFP* BAC reporter mice can be performed through direct eGFP visualization of tail snips (data not shown). Southern blot analysis was performed using standard Southern blotting procedures. The exon 1 probe used to label all blots was PCR amplified from the RP24-370G12 BAC clone, using the following primers: forward, 5′-TTCTTCCTCCCTTTTTTCTCCG-3′, and reverse, 5′-TTCTGCTCCA TCAGTCTCCACAG-3′. The *Rb* and *p130* conditional knockout alleles, the *p107* constitutive knockout allele, and the $Rosa26^{CreERT2}$ knock-in strain were described previously (39, 51, 52). $Rosa26^{CreERT2}$; $Rb^{lox/lox}$; $p130^{lox/lox}$; $p107^{-/-}$; *Rb BAC-eGFP* mice and all derivative genotypes are maintained in a mixed 129Sv/J:C57BL/6/J:DBA/2J background enriched for 129Sv/J and C57BL/6J. Mice are maintained according to practices prescribed by the NIH and are housed in Stanford's Research Animal Facility, accredited by the AAALAC.

Tamoxifen injections. Young-adult mice were injected with tamoxifen, 2 mg per injection, given as five consecutive intraperitoneal injections. Tamoxifen was resuspended in 100% ethanol at a concentration of 100 mg/ml. Once it was dissolved, corn oil was added to bring the final concentration to 10 mg/ml. The solution was sonicated for 1 min before being injected. Mice were injected with 200 μl of this solution. Mice were euthanized 3 days after the last injection. In unpublished observations related to a previous study (8), we found that injection of tamoxifen alone in $Rosa26^{CreERT2}$ mice led to more variable expression of a GFP transgene than corn oil injection in mice without the *CreER* knock-in allele. We never found any leaky Cre activity in $Rosa26^{CreERT2}$ mice in the absence of tamoxifen (52 and data not shown). These observations led us to use $Rosa26^{CreERT2}$-negative mice injected with tamoxifen as a more-stringent control in our experiments. We have previously found that the health of animals deteriorates 2 to 3 weeks after deletion of the RB family, as mice rapidly lose weight from potential digestive defects (52). Therefore, animals were euthanized 1 week after the first tamoxifen injection, at a time point when the TKO mice were visually indistinguishable from the control animals and had not begun to lose weight. Complete blood counts and blood chemistries showed no significant differences between TKO and control mice except for higher levels of some liver enzymes (such as aspartate amino transferase and alanine transaminase), which is consistent with increased proliferation in this organ. Analysis of electrolytes found in the blood further demonstrated that the TKO mice were neither dehydrated nor starving due to digestive defects at this time.

FACS. For initial FACS analysis *in vivo*, whole organs were mechanically ground and filtered through a 40-μm cell strainer. Whole-organ FACS analysis was performed, using a BD FACSCalibur instrument. For lineage-specific analysis, splenocytes were filtered and red blood cells were lysed with ACK buffer (NH4Cl-KHCO3). Mature white blood cells were subsequently stained with fluorochrome-conjugated antibodies against B220, Mac1, Gr1, CD3, or Ter119 for 30 min in the dark. All the antibodies were purchased from eBioscience. Analysis was performed at the Stanford Shared FACS Facility on a BD LSRII instrument, using CellQuest software for data acquisition (Becton Dickinson). Data were analyzed using FlowJo software (Tree Star). Sorting was performed at the Stanford Shared FACS Facility on a Vantage machine. Cells for mRNA analysis were sorted directly into Trizol; cells sorted for BrdU analysis were sorted into 10% serum and then fixed in 70% ethanol overnight.

For cell cycle analysis in MEF and sorted splenocyte populations, flow cytometry was carried out as described previously (36) and analyzed using a FACSCalibur instrument. The BrdU pulse was 4 h. For cell cycle analysis in MCF7

Downloaded from https://journals.asm.org/journal/mcb on 24 February 2022 by 2a01:4f9:3b:1ae9::

cells, flow cytometry was carried out as described previously (6). Prior to being harvested, cells were pulsed with BrdU (GE Healthcare Life Sciences) for 1 h and then were trypsinized and washed with PBS. Cells were washed once with PBS and with labeling buffer (1× PBS–2% serum–0.05% Tween 20) and then were incubated with anti-BrdU-FITC (BD Biosciences) for 45 min. After being washed two times, cells were immediately analyzed for BrdU uptake, using flow cytometry.

Immunostaining and immunoblotting. Mouse organs were fixed in 4% paraformaldehyde for 4 to 8 h at room temperature and then transferred to 30% sucrose overnight. Organs were then embedded and frozen in OCT, using liquid-nitrogen-cooled isopentane. For immunostaining, cryosections were dried at room temperature, briefly washed in PBST, and then blocked for 1 h at room temperature in PBST with 5% normal horse serum (eGFP single staining) or normal goat serum (double staining) and 1% BSA. Sections were incubated with primary antibodies diluted 1:200 in block solution overnight at 4°C, washed in PBST, and then incubated with secondary antibodies diluted 1:200 in block solution for 1 h at 37°C. Primary antibodies used were rabbit anti-GFP (A11122; Molecular Probes) and mouse anti-glutamine synthetase (BD Biosciences). For detection of RB in MCF7 cells by immunoblotting, 50 μg of total-cell extract from each growth condition was subjected to SDS-PAGE. The blots were probed with an anti-RB antibody (BD Pharmingen) and stripped and reprobed with anti-lamin B (M-20). The signals were normalized to the respective lamin B loading controls.

Microscopy. Tail biopsies and whole embryos were visualized, using a Leica MZFLIII dissecting scope. Generally, immunohistochemical analysis was performed using a Leica DM LB. Confocal analysis of the retinas was performed using a Leica SP2 DMIRE2 inverted confocal microscope.

Quantitative RT-PCR. Organs were snap-frozen in liquid nitrogen and then ground with a liquid-nitrogen-cooled mortar and pestle. RNA was extracted with Trizol (Invitrogen) and cleaned, using a Qiagen RNeasy kit. Up to 1 μg of RNA was reverse transcribed, using a New England Biolabs cDNA DyNAmo synthesis kit. TaqMan quantitative PCR was performed, using Eurogentec master mix. For cell cycle genes, SYBR GreenER master mix (Invitrogen) was used. *GFP* and *p107* primer/probes were described previously (8). All relative expression analyses were calculated relative to *TBP* (TATA binding protein) expression. The primers and probes used were as follows: for *Rb*, forward primer, 5′-ACTCCG TTTTCATGCAGAGACTAA-3′, reverse primer, 5′-GAGGAATGTGAGGTA TTGGTGACA-3′, and probe, 5′-FAM-CAGTATGCCTCCACCAGGCCTCC TACC-BHQ-3′; for *Rb* delta (*Rb* with a deletion of the conditional allele), forward primer, 5′-GGAGAAAGTTTCATCCGTGGAT-3′, reverse primer, 5′-GTGAATGGCATCTCATCTAGATCAA-3′, and probe, 5′-FAM-GGGCATC TGCATCTTTATCGCAGCA-BHQ-3′; for *p130* delta (*p130* with a deletion of the *p130* conditional allele), forward primer, 5′-GGACCGCTGAAGGAAACT ATGT-3′, reverse primer, 5′-CTTCCCACTTCTTCATCTTGTTAAAA-3′, and probe, 5′-FAM-CCTTCGCTGTTCGGAGCAGAGCCTAA-BHQ-3′; for *TBP*, forward primer, 5′-ACTTCGTGCAAGAAATGCTGAAT-3′, reverse primer, 5′-CAGTTGTCCGTGGCTCTCTTATT-3′, and probe, 5′-FAM-CCCAAGCG ATTTGCTGCAGTCATCAT-BHQ-3′; for *Cyclin E*, forward primer, 5′-CTGA GAGATGAGCACTTTCTG-3′, and reverse primer, 5′-GAGCTTATAGACTT CGCACACCT-3′; for mouse *Cdc6*, forward primer, 5′-GTTCTGTGCCCGCA AAGTG-3′, and reverse primer, 5′-AGCTCGCCTGCAAACATCC-3′; for human *Cdc6*, forward primer, 5′-GGCACAGGCTACAATCAGTT-3′, and reverse primer, 5′-AATCTCCTGAGCAATAGCT-3′; for human *RB*, forward primer, 5′-AGGATCAGATGAAGCAGATGG-3′, and reverse primer, 5′-TGC ATTCGTGTTCGAGTAGAAG-3′; and for human *TBP*, forward primer, 5′-G CTGGCCCATAGTGATCTTT-3′, and reverse primer, 5′-CTTCACACGCCA AGAAACAGT-3′.

RNA was isolated from the harvested MCF7 cells, using Trizol. Five micrograms of total RNA was reverse transcribed, using random hexamers and SuperScript III reverse transcriptase (Invitrogen). One hundred fifty nanograms of cDNA was PCR amplified with *RB* mRNA primers (forward primer, 5′-GGAA GCAACCCTCCTAAACC-3′; reverse primer, 5′-TTTCTGCTTTTGCATTCGT G-3′) or *GAPDH* mRNA primers (forward primer, 5′-TGGAAATCCCATCACC ATCT-3′; reverse primer, 5′-TTCACACCCATGACGAACAT-3′). Expression in MCF7 cells was calculated relative to *GAPDH* expression.

Using primers located in *Rb* exon 22, listed above as *Rb*, we observed that *Rb* mRNA sequences downstream of exon 3 are still expressed in cells that have a deletion of exon 3, although no protein is made from this transcript (39). To accurately quantify *Rb* expression and the efficiency of deletion in conditional mutant mice, we designed a PCR protocol employing one oligonucleotide in *Rb* exon 3 (52), the primers listed above as *Rb* delta. Using these primers, we also found that *Rb* mRNA sequences downstream of the polyadenylation site in the *eGFP* cassette are variably expressed in transgenic mice. Thus, our strategy to quantify the decrease in *Rb* expression upon Cre-mediated deletion has been to perform RT-qPCR for analysis of *Rb* deletion in littermates of *Rb-eGFP*; $Rb^{lox/lox}$; $Rosa26^{CreERT2}$ mice that do not harbor the *eGFP* transgene.

gDNA was extracted from frozen tissues and resuspended at a concentration of 50 ng/μl. Quantitative PCR was performed on gDNA, using SYBR GreenER master mix (Invitrogen) and the *Rb* and *p130* genotyping primers described above. Quantification was performed relative to the wild-type *p53* locus, using forward primer 5′-CACAAAAACAGGTTAAACCCAG-3′ and reverse primer 5′-AGCACATAGGAGGCAGAGAC-3′.

Luciferase assays. To construct the plasmid reporters, primers were designed to amplify the *Rb* and *p107* promoters from mouse BAC clones (RP24-370G12 and RP23-163J20, respectively) to enable cloning directly into the multiple-cloning site of PGL3-basic (Promega). The reverse primers were positioned to include all sequences upstream of the translation start site. Point mutations in the *Rb* promoter, changing the TTTCCCGC sequence to TTTACATC (point mutations are indicated by underlining), were introduced to generate the Rb^{E2Fmut} construct (additional details available upon request). MEFs (10^4) were plated in wells of 48-well plates and transfected 1 day later. Luciferase activity was measured 2 days after the transfection according to the manufacturer's instructions (Promega). In all luciferase assays, 500 ng of each luciferase construct was cotransfected with 125 ng of a *Renilla* luciferase vector. For exogenous E2F3 experiments, 100 ng of DP1 was cotransfected with either 100 ng of pCDNA empty vector or 100 ng of CMV-E2F3. Transfections were carried out using Fugene 6 (Roche).

Statistics. Statistical significance was assayed by Student's *t* test. The mean and standard error of the mean of the results of each experiment are shown in the figures. An asterisk indicates that $P \leq 0.05$.

RESULTS

RB family members bind directly to the *RB* promoter. Increasing evidence, including the presence of a conserved E2F binding site in the proximal promoter region (Fig. 1a), suggests that E2F family members may control *RB* transcription in mammalian cells (1, 15, 30, 33, 43). Similar to what has previously been shown (56), we found that E2F4, an E2F family member involved in gene repression, binds directly to the proximal promoter of the *Rb* gene in ChIP assays with immortalized MEFs (Fig. 1b). Because RB family members are normally required to localize E2F4 in the nuclei of cells (49), this observation suggests that RB, p107, and/or p130 may bind to the *Rb* promoter and control its activity. Indeed, we found that p107 and p130 bind directly to the mouse *Rb* promoter in ChIP assays (Fig. 1b). Detection of endogenous RB binding to target gene promoters has proven challenging (47, 50), and we were unable to detect RB binding to the *Rb* promoter in immortalized MEFs (data not shown). In order to investigate the ability of RB to directly regulate its own promoter, we took advantage of a recently described GFP-RB fusion, which is functional when expressed in mammalian cells and can be detected using GFP antibodies (47). Using this construct, we found that RB was able to bind to the proximal human *RB* promoter in Saos2 cells (Fig. 1c, left panel). Similarly, GFP-p107 and GFP-p130 molecules bound directly to the human *RB* promoter in these cells (Fig. 1c, middle and right panels). These experiments indicate that RB family members bind directly to the *RB* promoter, suggesting that RB, p107, and/or p130 may regulate *RB* transcription, at least in certain contexts.

RB expression does not change with cell cycle progression, unlike that of classical E2F target genes. The binding of RB and E2F family members to the *RB* promoter raised the question of whether *RB* was a cell cycle-regulated gene. To answer this question, we examined *RB* mRNA levels during cell cycle progression. First, we expanded and stained immortalized MEFs with Hoechst 33342, a DNA-intercalating agent that

Downloaded from https://journals.asm.org/journal/mcb on 24 February 2022 by 2a01:4f9:3b:1ae9::

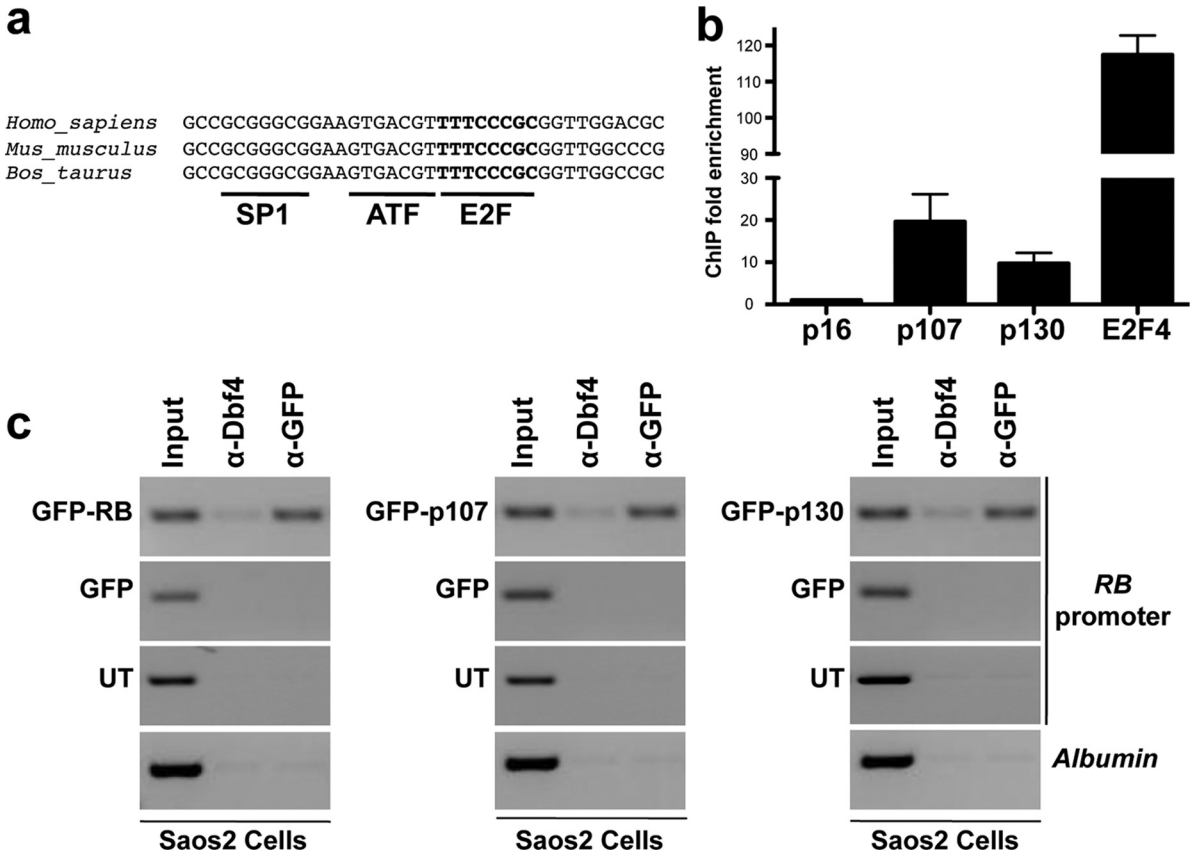

FIG. 1. Direct binding of RB family members to the *RB* promoter. (a) Conservation of binding sites for the SP1, ATF, and E2F (bold) transcription factors in the proximal *RB* promoter. (b) Quantitative ChIP analysis of p107, p130, and E2F4 on the *Rb* promoter in NIH3T3 fibroblasts ($n = 2$). Enrichment is calculated over an unrelated DNA sequence (*Actin*) and normalized to the binding to a negative-control antibody (p16). (c) Representative ChIP analysis of GFP-RB, GFP-p107, and GFP-p130 fusion proteins on the *RB* promoter in Saos-2 cells. Untransfected (UT) cells and cells transfected with GFP serve as negative controls. ChIP was performed using GFP antibodies as well as antibodies for Dbf4 as negative controls. Input and immunoprecipitated DNA were amplified by PCR with primers specific for the human *RB* promoter and one non-E2F target gene (*Albumin*).

enabled the cells to be sorted by FACS by DNA content. RT-qPCR analysis showed that *Rb* RNA levels were similar in quiescent MEFs and in G_1- and S-phase populations of asynchronously cycling MEFs sorted by FACS, while the expression of both classical E2F target genes *p107* and *Cdc6* increased as a function of the cell cycle (Fig. 2a). Because control of *RB* may vary in different cell types and species, we next synchronized human T98G glioblastoma cells in G_0 by serum starvation; 15 h after induction of cell cycle reentry by the addition of a 20% concentration of serum, cells had entered the late G_1 phase of the cell cycle, judging by the increased expression of *CDC6*, a direct E2F target involved in DNA replication (23) (Fig. 2b), and by PI staining for DNA content (data not shown). In contrast, at the same time point, *RB* levels remained similar to those found in quiescent cells (Fig. 2b).

We next investigated the potentially dynamic binding of E2F and RB family members to the *RB* promoter as a function of the cell cycle through ChIP analysis of synchronized T98G cells. It has previously been shown that in these cells, the promoters of classical E2F target genes, such as *CDC6*, are generally bound by repressing complexes containing E2F4 and p130 during G_0 and by activating E2Fs 1 to 3 during late G_1 (48); we observed a similar pattern in our experiments (Fig. 2c and d). We found that E2F1, E2F3, E2F4, p107, and p130 all bound the proximal *RB* promoter both in G_0 and 15 h after the addition of serum (Fig. 2c and d). There was a trend for more activating E2Fs (E2F1 and E2F3) to bind the *RB* promoter in G_1/S, while E2F4 and p130 bound more in G_0 (Fig. 2c and d). We also examined the binding of SP1 and ATF, two other potential regulators of *RB* transcription (1, 41) (Fig. 1a), and found that both bound the *RB* promoter in quiescent and cycling cells (Fig. 2d).

Finally, in order to further determine whether the *Rb* promoter was responsive to E2F activity, we utilized a luciferase reporter assay. We found that a 1,100-bp fragment of the mouse *Rb* promoter encompassing the consensus E2F binding site was not induced by expression of E2F3 in wild-type MEFs, while a similar *p107* construct responded as expected (39, 58) (Fig. 2e). These data further support the notion that *Rb* is not a classical E2F target gene. Interestingly, however, the same *Rb* promoter fragment could be induced by ectopic E2F3 expression in $Rb^{-/-}$ MEFs. Surprisingly, mutation in the consensus E2F binding site did not abolish this induction (Fig. 2e, lower panel). In these experiments and previously published

Downloaded from https://journals.asm.org/journal/mcb on 24 February 2022 by 2a01:4f9:3b:1ae9::

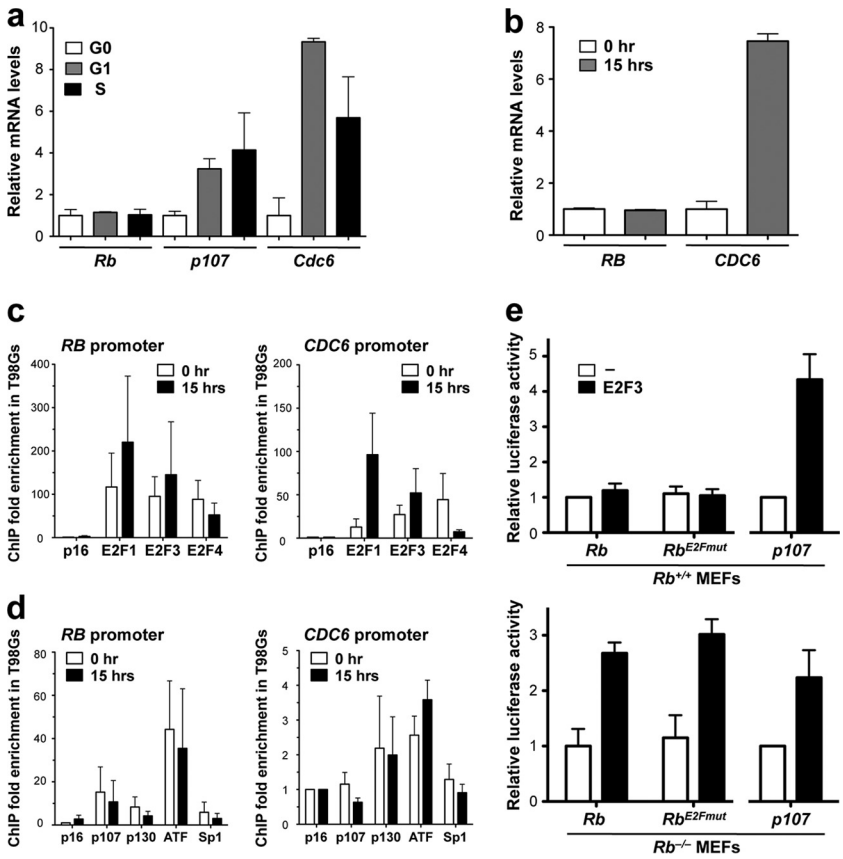

FIG. 2. Regulation of *RB* transcription is not cell cycle dependent. (a) RT-qPCR of mouse *Rb*, *p107*, and *Cdc6* mRNA in asynchronously cycling immortalized MEFs. G_1- and S-phase cells were sorted by DNA content through Hoechst staining and compared to samples rendered quiescent through 3 days of serum starvation (G_0) ($n \geq 2$). (b) RT-qPCR of human *RB* and *CDC6* in quiescent (0 h) T98G cells and cells synchronized in G_1/S phase (15 h). Hours are times poststimulation with 20% serum ($n = 2$). (c and d) Quantitative ChIP of E2F family binding (c) and ATF, Sp1, and RB family binding (d) to the *RB* (left panels) and *CDC6* (right panels) promoters in quiescent (0 h) and G_1/S-phase (15 h) T98G cells. Antibodies used for ChIP are indicated ($n = 3$). (e) Wild-type (upper panel) and *Rb* null (lower panel) MEFs were cotransfected with luciferase constructs for the *Rb* and *p107* promoters and with an empty expression vector (−) or a vector expressing E2F3 (E2F3) ($n = 3$). The Rb^{E2FMut} construct represents the *Rb* promoter carrying a mutation in the E2F site. The break in the *x* axis indicates that the luciferase activities were normalized to each wild-type construct cotransfected with the empty vector.

ones, we found that the cell cycle status of *Rb* wild-type and mutant cells was not significantly different (39, 40; also data not shown). These observations suggest that the presence of RB may inhibit the E2F-dependent activity of the *Rb* promoter. In addition, these experiments suggest that the *Rb* promoter may be responsive to E2F activity under certain conditions but that responsiveness is either indirect or dependent on an uncharacterized E2F binding site in the promoter region.

Together, these experiments in culture show that RB and E2F family members bind the proximal *RB* promoter but also indicate that *RB* is not a classical E2F target gene whose expression changes with the cell cycle. Other factors that are known to bind to and mediate the effects of RB on transcription, such as SP1 and ATF (26, 27), also directly bind the *RB* promoter. These observations led us to investigate the intriguing possibility that RB family members may control *RB* expression, at least in certain contexts, including in different cell types *in vivo*.

***eGFP* expression largely parallels endogenous *Rb* expression in *Rb-eGFP* BAC transgenic reporter mice.** In order to investigate the regulation of *RB* expression by RB family members *in vivo*, we sought to develop a tool that would allow us to track changes in the transcription of the mouse *Rb* mRNA in cells, including cells with genetic inactivation of the *Rb* gene itself. We chose a transgenic reporter approach, rather than a knock-in of the reporter into the endogenous *Rb* gene in order to prevent any effects of *RB* haploinsufficiency (31, 57). Transgenic mice have been generated previously, using *RB* promoter regions to drive reporter gene expression. In these mice, 6 kb or less of human and mouse upstream regulatory sequences were used to drive *lacZ* expression in the developing embryo, but this was insufficient to reflect endogenous *Rb* expression in several cell types (1, 24). We surmised that longer regulatory sequences would result in a more accurate expression of a reporter gene. To test this idea, we used recombineering in bacteria to knock-in an *eGFP* cassette at the start codon of *Rb* in a BAC containing 180 kb of genomic sequence centered around the transcription start site of *Rb* (Fig. 3a). The *eGFP* reporter construct also included two polyadenylation signals that prevent downstream expression of the coding *Rb* transcript from the BAC (Fig. 3b).

Injection of *Rb-eGFP* BAC DNA into fertilized mouse oo-

Downloaded from https://journals.asm.org/journal/mcb on 24 February 2022 by 2a01:4f9:3b:1ae9::

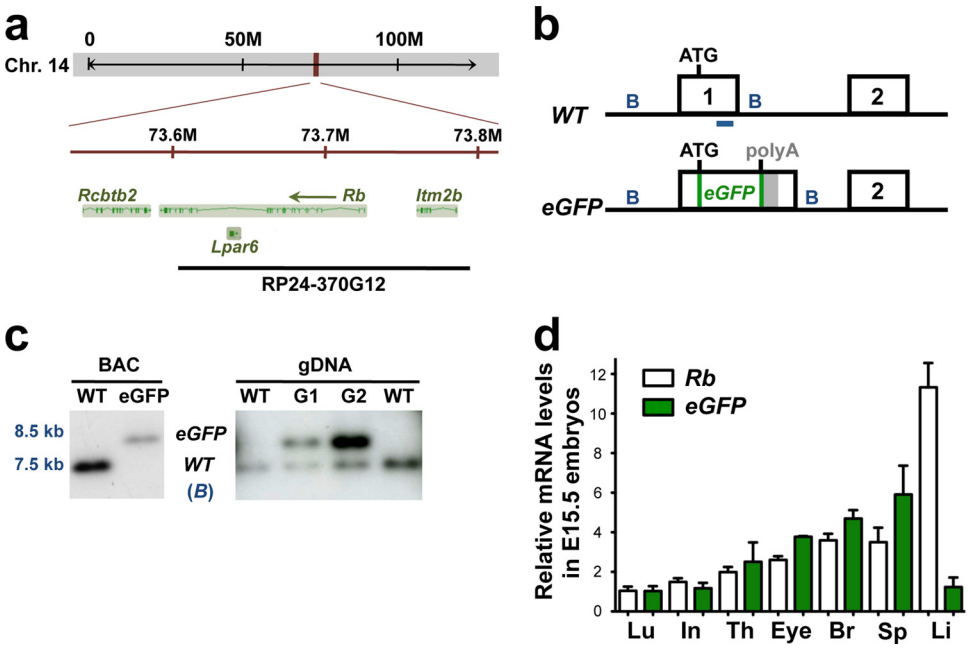

FIG. 3. Generation of *Rb-eGFP* transgenic mice. (a) The RP24-370G12 mouse BAC is located 73.7 Mb from the origin of chromosome 14. This BAC encompasses more than 50 kb upstream of *Rb* and more than 100 kb downstream of *Rb*, but it does not contain the final coding exons. Two other cellular genes (*Lpar5* and *Itm2b*) are contained within the BAC sequences, while a third (*Rcbtb2*) is outside of the BAC. (b) Schematic representation of the *Rb* BAC knock-in reporter. The *eGFP* cDNA is inserted at the ATG in exon 1 of *Rb*. The *eGFP* cassette contains two polyadenylation (polyA) sequences. Boxes indicate *Rb* exons 1 and 2, and B indicates BamHI. The location of the probe used in Southern blot experiments is indicated below exon 1. (c) Southern blot analysis of *Rb* 5′ regulatory sequences in the gDNA of *Rb-eGFP* BAC transgenic mice. BamH1 (B)-digested BAC DNA extracted from bacteria serves as a size control. gDNA from the two founder lines (G1 and G2) was analyzed. (d) Analysis by RT-qPCR of *Rb* and *eGFP* expression in organs collected from E15.5 *Rb-eGFP* transgenic embryos. mRNA expression for each gene was calculated relative to levels in the lung ($n = 2$). Lu, lung; In, intestine; Th, thymus; Br, brain; Sp, spleen; Li, liver.

cytes generated two independent founder lines. These transgenic mice were viable and fertile. The BAC-containing *Rb* sequence does not encompass the entire coding sequence for the RB protein, and the transgenic mice did not display any of the growth phenotypes of mice with increased levels of RB (32), indicating that no functional protein was made from the reporter transgene. Southern blot analysis confirmed that at least 7.5 kb of the 5′ regulatory sequence immediately upstream of the translation start site and 12.4 kb of the 3′ regulatory sequence downstream of the translation start site were intact within the genome of cells from these transgenic mice (Fig. 3c and data not shown). Preliminary experiments demonstrated that both lines had similar eGFP expression patterns; the experiments shown here were performed with the line with more copies of the transgene (line G2), except when noted otherwise. As a first test to determine whether *Rb-eGFP* BAC transgenic mice could be used to monitor *Rb* transcription, we examined *eGFP* expression in organs from transgenic embryos 15.5 days after fertilization (E15.5). RT-qPCR analysis showed that *eGFP* expression paralleled that of *Rb* in most of the organs surveyed (Fig. 3d), with the notable exception of the embryonic liver.

Using immunostaining, we next found that the reporter was strongly expressed in the developing central nervous system of early- and mid-gestation embryos (Fig. 4a and b) in a pattern largely similar to what has been observed by *in situ* hybridization for the *Rb* mRNA (25) and in other reporter strains (1, 24). These previous transgenic reporter systems did not reflect *Rb* expression in muscle cells (1, 24), but *eGFP* is strongly expressed in skeletal and cardiac muscle cells in *Rb-eGFP* BAC transgenic embryos (Fig. 4b and c). High levels of *Rb* have previously been observed in the embryonic liver by *in situ* hybridization (25); however, we detected only low levels of eGFP in this tissue in transgenic embryos (Fig. 3d and 4b and c). We next examined the expression of eGFP in E17.5 embryos, 1 day before birth, and found that the reporter was expressed at high levels in the vibrissae (Fig. 5a and b), the thymus (Fig. 5c), and the developing musculature, including the tongue (Fig. 5d and data not shown), as was determined previously by *in situ* hybridization for the *Rb* mRNA (25). Overall, despite a discrepancy in expression in the liver, *eGFP* expression in *Rb-eGFP* embryos closely mimics that of the *Rb* gene (25).

RT-qPCR performed on RNA from a selection of adult mouse organs showed that *Rb* mRNA expression varied, with the lowest levels observed in the liver and higher levels observed in the heart and muscle (Fig. 6a, white bars). Similar analysis of the *eGFP* mRNA in the *Rb-eGFP* BAC reporter mice showed that *eGFP* expression largely represented that of endogenous *Rb* in many organs, but not in the thymus and the kidney (Fig. 6a).

In order to further validate the use of our *eGFP* reporter as a marker for *Rb* transcription, we next sought to sort different subpopulations within the blood compartment. We observed through pilot experiments that splenic B cells and T cells expressed different levels of eGFP during FACS analysis (Fig. 6b

Downloaded from https://journals.asm.org/journal/mcb on 24 February 2022 by 2a01:4f9:3b:1ae9::

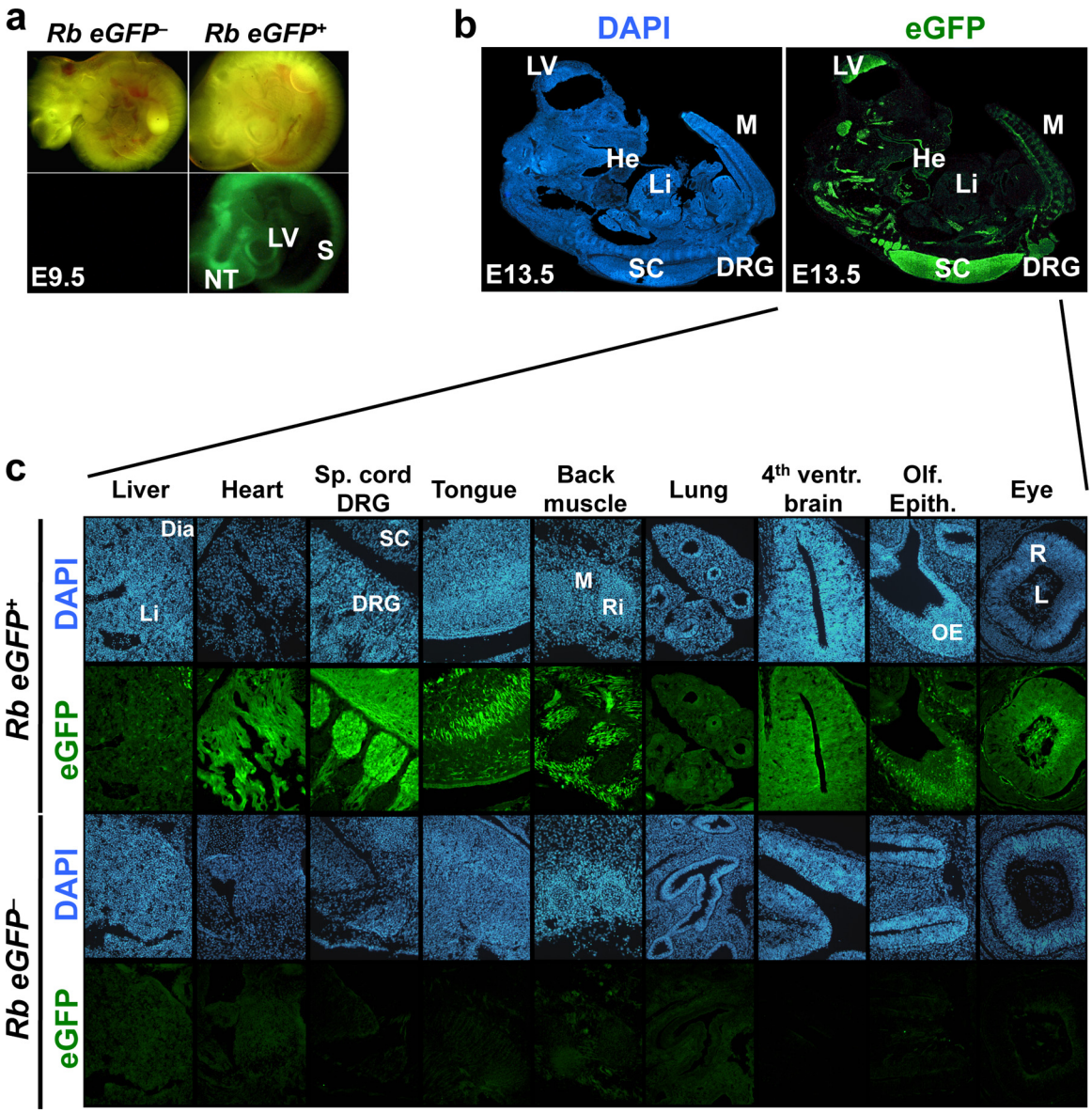

FIG. 4. *eGFP* expression in *Rb-eGFP* transgenic mice largely mimics *Rb* expression in early- and mid-gestation embryos. (a) Direct visualization of eGFP in an *Rb-eGFP* embryo at E9.5. NT, neural tube; LV, lateral ventricle; S, somites. (b) Immunofluorescence analysis of eGFP expression in E13.5 transgenic embryos. He, heart; Li, liver; SC, spinal cord; M, muscle; DRG, dorsal root ganglia. DAPI marks the DNA in blue. (c) Immunofluorescence analysis of eGFP in *Rb-eGFP* embryos (*Rb eGFP*$^+$) in different organs at E13.5. *Rb-eGFP*$^-$ embryos serve as negative controls. R, retina; L, lens; OE, olfactory epithelium; Ri, ribs; Dia, diaphragm muscle. Magnification, ×400.

and data not shown). We sorted these two populations from *Rb-eGFP* transgenic mice and examined *Rb* mRNA expression within these cells. We observed that B cells, which express higher levels of eGFP when analyzed by FACS, express nearly twofold the amount of *Rb* mRNA observed in T cells (Fig. 6b).

Expression of *RB* in the retinas of adult mice and humans has been previously examined by *in situ* hybridization and immunostaining and found to be at higher levels in the inner nuclear layer and the ganglion cell layer; RB levels are consistently high in Müller glia cells, in particular (16, 45). We found that *eGFP* was broadly expressed in the adult mouse retina, with higher levels in the inner nuclear layer and the ganglion cell layer. Immunostaining for glutamine synthetase, a marker of Müller glia cells, showed that eGFP colocalizes with this marker in the transgenic mice (Fig. 6c). Thus, the overall pattern of *eGFP* expression in the retina is similar to what has been previously observed for endogenous *Rb*. We also found that the transgene was expressed at high levels in Purkinje cells of the cerebellum in adult mice (Fig. 6d), similar to what was shown by immunostaining for RB on adult human brain sections (11).

Together, these observations indicate that *Rb-eGFP* BAC mice represent a faithful reporter strain to follow *Rb* transcription in mouse organs and tissues. These data also suggest that long-distance enhancers and/or posttranscriptional mechanisms control the levels of *Rb* mRNA in certain cell types, including embryonic liver, adult thymus, and adult kidney.

Downloaded from https://journals.asm.org/journal/mcb on 24 February 2022 by 2a01:4f9:3b:1ae9::

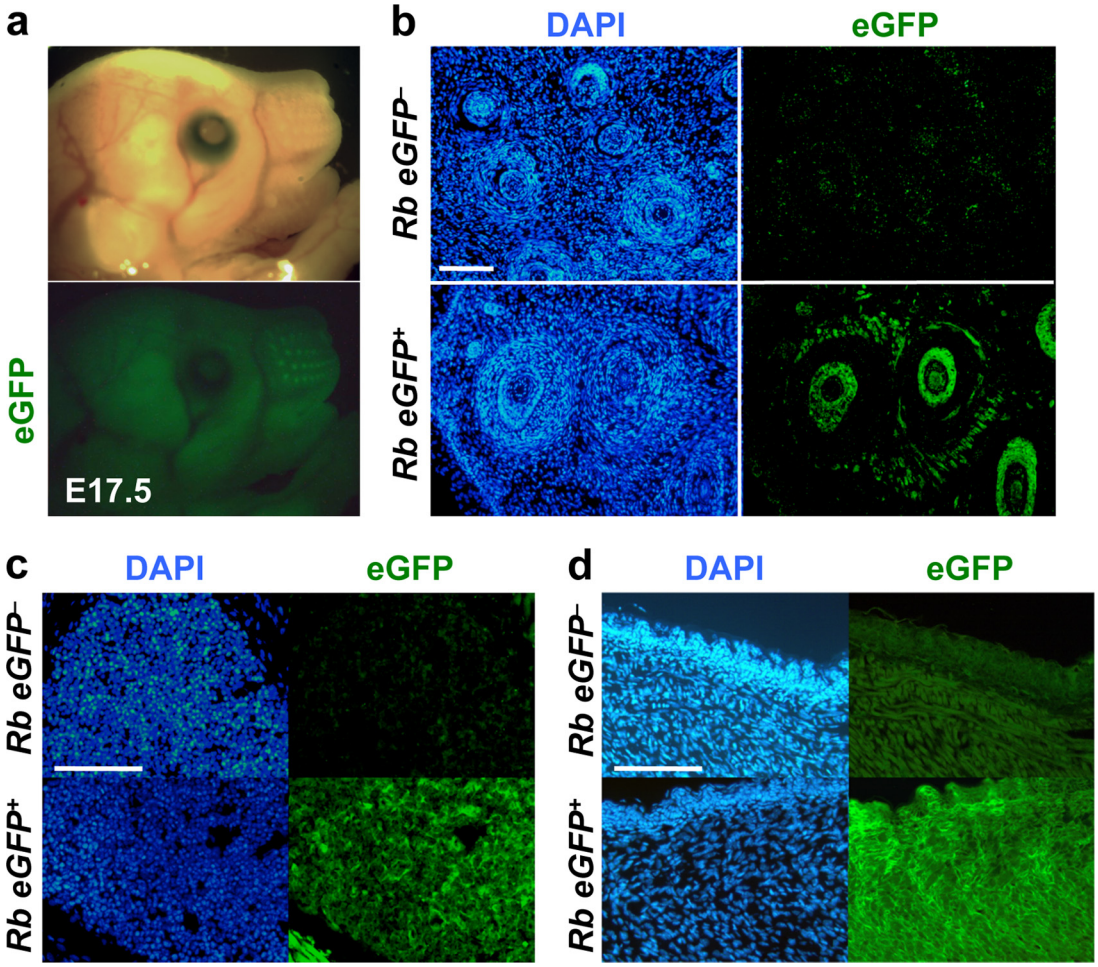

FIG. 5. *eGFP* expression in *Rb-eGFP* transgenic mice largely mimics *Rb* expression in late embryos. (a) Direct visualization of eGFP in the head region of an *Rb-eGFP* embryo at E17.5. Expression in the brain and in vibrissae is visible. (b to d) Immunofluorescence analyses of eGFP expression in sections of the vibrissae (b), the thymus (c), and the tongue (d) of a representative E17.5 transgenic embryo. Each time, a section from a control embryo (*Rb eGFP*$^{-}$) is shown. Bar, 100 μm.

Cell-type-specific autoregulation of *Rb* expression by RB in culture and *in vivo*. To examine the potential role of RB autoregulation, we crossed *Rb-eGFP* BAC transgenic mice to *Rb* conditional mutant mice (*Rb*$^{lox/lox}$) and *Rosa26*^{CreERT2} mice, in which Cre activity can be induced in a broad number of cell types *in vivo* by tamoxifen injection. We first produced *Rb-eGFP*; *Rb*$^{lox/lox}$ MEFs from these mice and infected these MEFs with an adenovirus expressing the Cre recombinase (Ad-Cre) to delete the conditional *Rb* alleles (Fig. 7a and b). We found that *eGFP* levels were slightly lower in quiescent and asynchronously cycling *Rb-eGFP*; *Rb*$^{\Delta/\Delta}$ MEFs (where Δ represents the deleted *Rb* allele [Fig. 7a]) compared to those in the controls; *p107* levels increased upon loss of *Rb*, as expected (Fig. 7b) (39). In light of our luciferase results suggesting that E2F may activate the *Rb* promoter in the absence of RB, we next performed cell cycle reentry experiments with wild-type and *Rb*-deficient cells. We found that *eGFP* levels mimicked *Rb* levels in wild-type MEFs reentering the cell cycle, with a decrease in expression 8 h after serum stimulation and a slight increase at the next time points (12 to 24 h of stimulation). At all these time points, we found that *eGFP* levels were lower in *Rb* mutant cells compared to those in the control cells (Fig. 7c). As expected, expression of *Cdc6* increased as cells reentered the cell cycle and increased even more in *Rb* mutant cells 8 h after serum stimulation (Fig. 7d). Thus, the absence of RB in primary MEFs generally results in a small decrease in the transcriptional activity of the *Rb* promoter. This observation indicates that RB normally activates its own promoter in MEFs. While these experiments do not address whether this is a direct effect, the fact that the decrease in *Rb* transcription in *Rb* mutant cells is found at all stages of the cell cycle indicates that this is likely a cell cycle-independent phenomenon.

We next investigated whether loss of *Rb* may alter *Rb* expression *in vivo* by measuring the levels of *eGFP* in various mouse organs. We focused on organs in which the deletion of *Rb* was most efficient, resulting in reduced expression of *Rb*, and for which the expression of the reporter faithfully represented *Rb* expression: the liver, the lungs, and the spleen (Fig. 6a and 8a and b). While *Cyclin E*, *Cdc6*, and *p107* all increased in both the liver and the lungs of *Rb* mutant mice, the *eGFP* levels significantly increased only in the lungs; in the spleen, which showed a trend toward increased *eGFP* levels, the ex-

Downloaded from https://journals.asm.org/journal/mcb on 24 February 2022 by 2a01:4f9:3b:1ae9::

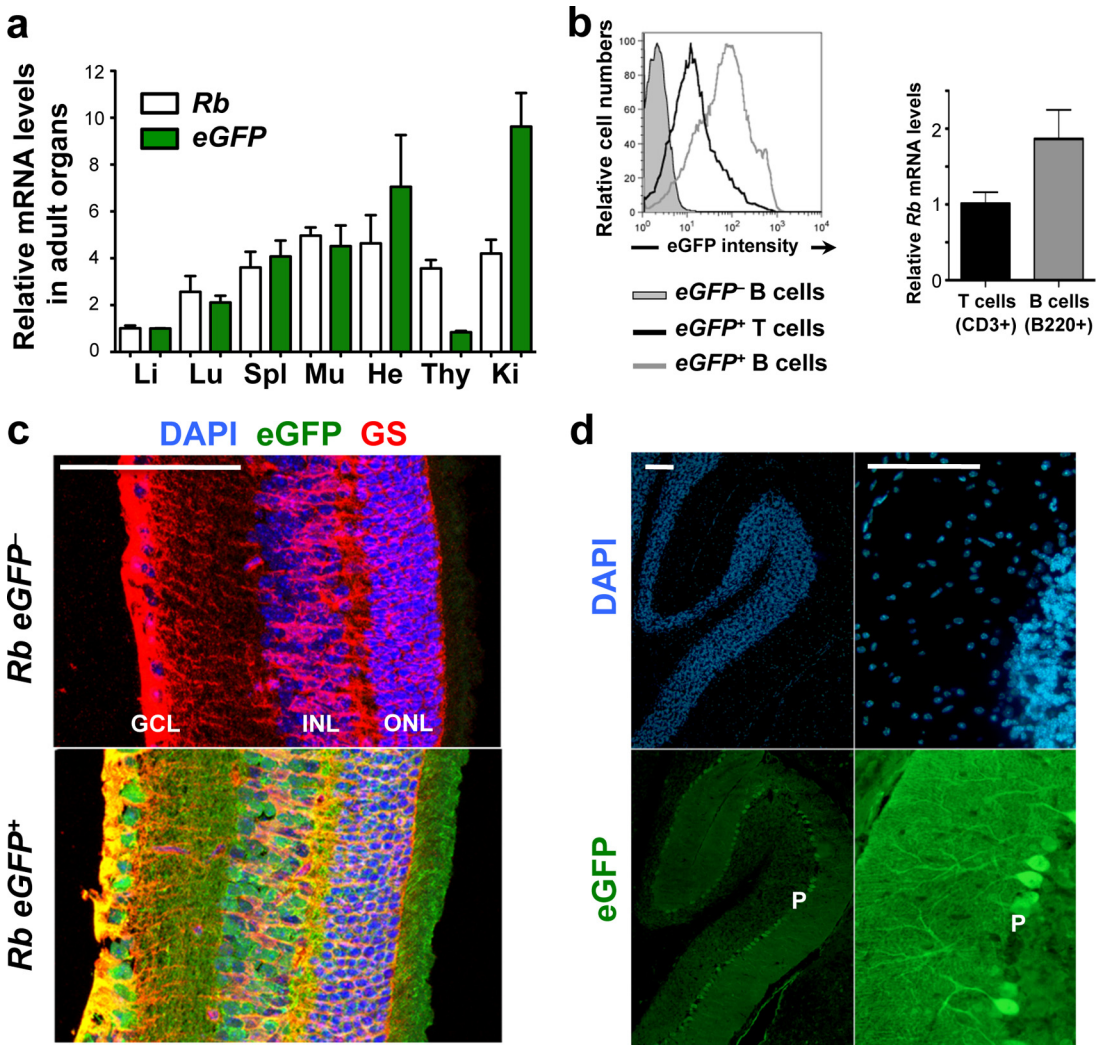

FIG. 6. *eGFP* expression in *Rb-eGFP* transgenic mice largely mimics *Rb* expression in adult mice. (a) Analysis by RT-qPCR of *Rb* and *eGFP* expression in organs collected from *Rb-eGFP* transgenic mice ($n \geq 2$). Data from line G1 are shown; similar data were obtained for line G2 (not shown). mRNA expression for each gene was calculated relative to that for the liver. Li, liver; Lu, lung; Spl, spleen; Mu, muscle; He, heart; Thy, thymus; Ki, kidney. (b) FACS analysis (left panel) of eGFP expression and RT-qPCR analysis of *Rb* mRNA expression (right panel) in B cells and T cells isolated from the spleens of wild-type *Rb-eGFP* transgenic mice. (c) Confocal immunofluorescence analysis of eGFP expression (green signal) and for the Müller glial cell marker α-glutamine synthetase (GS, red signal) in the retinas of *Rb-eGFP* transgenic (*Rb-eGFP*$^+$) and control (*Rb-eGFP*$^-$) mice. GCL, ganglion cell layer; INL, inner nuclear layer; ONL, outer nuclear layer. Bar, 100 μm. (d) Immunofluorescence analysis of eGFP expression in the cerebellum of an *Rb-eGFP*$^+$ mouse. P, Purkinje cells. Bars, 100 μm.

pression of the other cell cycle genes remained unchanged (Fig. 8c and d).

One explanation for the general lack of a more significant effect on the *Rb* promoter upon the deletion of the gene could be that the control of *Rb* by its own gene product is highly cell type and context dependent. In this case, changes in *Rb* levels in specific cell populations may be masked in the RNA isolated from a whole organ. We and others have found that the *Rb* gene family may play a critical role in various stages of the hematopoietic process, including in myeloid cells (42, 46, 52–54). Therefore, we next asked whether specific subpopulations of hematopoietic cells would display significant changes in *Rb* transcription upon loss of *Rb* function. We used cell surface markers to examine *eGFP* expression within three hematopoietic subpopulations within the adult mouse spleen, an organ in which *eGFP* expression closely mimics that of endogenous *Rb*. We reproducibly found that *eGFP* expression increased in *Rb* mutant Mac1$^+$/Gr1$^+$ myeloid granulocytes from *Rb-eGFP* mice compared to that in cells from *Rb* wild-type *Rb-eGFP* mice (Fig. 8e). On the other hand, no consistent change in eGFP expression was observed in other cell types examined, B cells and T cells (Fig. 8e and data not shown). RT-qPCR analysis indicated that in both Mac1$^+$/Gr1$^+$ myeloid cells and B cells, but not in T cells, classical target genes of the RB pathway such as *cyclin E*, *Cdc6*, and *p107* were increased in *Rb*-deficient cells. Together, these results suggest that RB normally represses its own transcription in some cell types *in vivo*, including myeloid cells. These data further show that depending on the cellular context, loss of RB may have different effects on *Rb* transcription—no effect, repression, or activa-

Downloaded from https://journals.asm.org/journal/mcb on 24 February 2022 by 2a01:4f9:3b:1ae9::

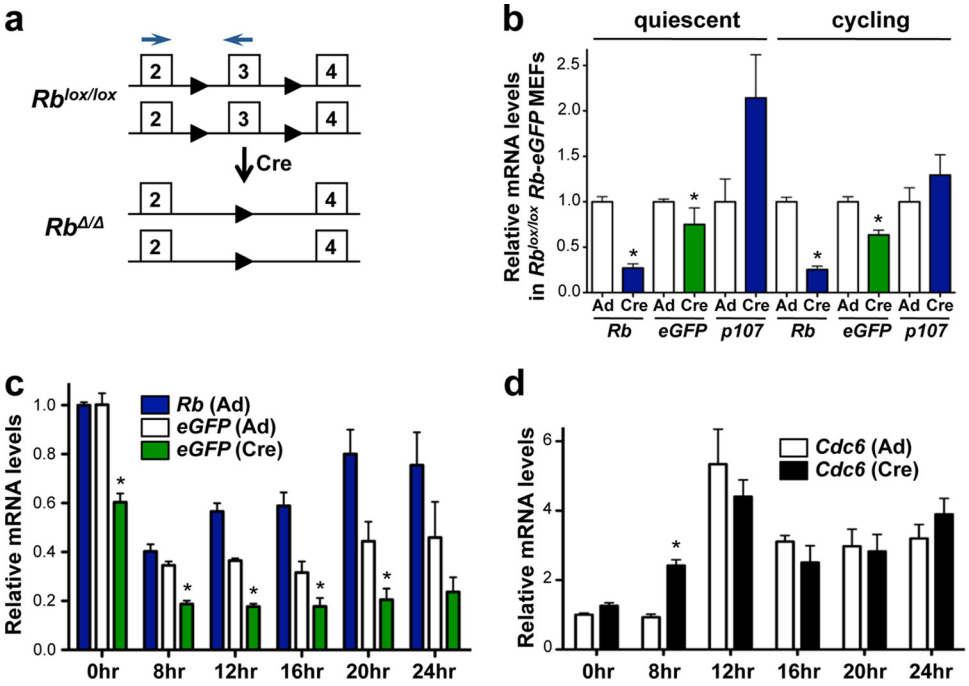

FIG. 7. *RB* positively regulates its own transcription in MEFs. (a) Schematic representation of the conditional Rb^{lox} allele. Blue arrows indicate locations of primers used to detect deletion of the *Rb* mRNA. Cre-mediated excision results in the genomic deletion of exon 3 and in the loss of *Rb* mRNA containing exon 3 sequences. (b) Analysis by RT-qPCR of *Rb* deletion (as for panel a) and *eGFP* and *p107* mRNA expression in $Rb^{lox/lox}$; *Rb-eGFP* MEFs infected with Adeno-Cre (Cre) relative to those for cells infected with a control adenovirus (Ad) ($n = 3$). (c and d) Analysis by RT-qPCR of *Rb*, *eGFP*, and *Cdc6* mRNA in $Rb^{lox/lox}$; *Rb-eGFP* MEFs infected with Adeno-Cre or a control adenovirus rendered quiescent through 3 days of serum starvation and then stimulated into synchronized cell cycle reentry through the addition of a 20% concentration of serum. Hours indicate time elapsed since the addition of serum ($n = 3$).

tion—and that these effects are different from the effects observed on classical E2F target genes within the same context.

Regulation of *Rb* expression by p107 and p130 *in vivo*. The presence of p107 and p130 at the *RB* promoter in mouse and human cells (Fig. 1 and 2) suggests that *Rb* expression may also be directly controlled by p107 or p130. However, when we examined *Rb* mRNA levels across a series of $p107^{-/-}$ adult mouse organs and tissues, we found no significant difference in *Rb* expression compared to that for the wild type (Fig. 9a). Similarly, we observed no changes in *eGFP* expression in organs and tissues from $p107^{-/-}$; *Rb-eGFP* mice (data not shown). We were also unable to detect any significant change in *Rb* expression levels in quiescent MEFs with a knockdown of *p107* (data not shown).

One possible reason why we observed that the absence of p107 had no effect on *Rb* mRNA levels in adult mice may be that the cells from these mice are constitutively deficient for p107 throughout development, allowing for transcriptional networks to compensate for its absence. While no tools for acute deletion of the *p107* gene *in vivo* currently exist, we have recently generated a conditional knockout allele for *p130* (Fig. 9b) (52). We crossed these $p130^{lox/lox}$ mice to the $Rosa26^{CreERT2}$ allele to be able to delete *p130* acutely in a broad number of cell types (51). We found that our protocol resulted in significant reductions in *p130* mRNA levels in various organs (Fig. 9c), but we did not detect any significant changes in *Rb* levels (Fig. 9d).

We then hypothesized that regulation of the *Rb* promoter by p107 or p130 may be highly dependent upon cellular context, much as we observed for RB autoregulation. To test this possibility, we again examined subpopulations within the spleen in which *Rb* transcription may be under the specific control of either p107 or p130. While there was no significant difference in *Rb* mRNA levels in wild-type versus $p107^{-/-}$ spleens (Fig. 9a), FACS analysis of $Mac1^+/Gr1^+$ splenic granulocytes showed a modest but reproducible increase of *eGFP* expression in $p107^{-/-}$; *Rb-eGFP* BAC mice compared to that in *Rb-eGFP* BAC mice (Fig. 9e). No changes in *eGFP* expression were found in other immune cells tested, including red blood cells, T cells, and B cells (data not shown). Interestingly, upon tamoxifen-induced deletion of the conditional $p130^{lox/lox}$ alleles, a slight decrease in eGFP levels in the same $Mac1^+/Gr1^+$ subpopulation was reproducibly detected, while the other immune cells tested remained largely unchanged (Fig. 9f and data not shown). Thus, loss of p107 or p130 results in modest changes in *Rb* transcription in specific cell populations *in vivo*.

Deregulation of the *Rb* promoter through loss of function of the RB pathway. The moderate effects observed upon the loss of the individual pocket proteins on *Rb* promoter expression could be the result of compensatory or overlapping functions between RB, p107, and p130. To test this idea, we generated $Rb^{lox/lox}$; $p130^{lox/lox}$; $p107^{-/-}$; $Rosa26^{CreERT2}$; *Rb-eGFP* mice (TKO), which allowed the examination of *Rb* transcription in response to the deletion of the entire *Rb* gene family simultaneously. We first infected $Rb^{lox/lox}$; $p130^{lox/lox}$; $p107^{-/-}$; *Rb-eGFP* MEFs with Adeno-Cre in culture in order to delete the conditional *Rb* and *p130* alleles alongside the *p107* null allele. Four

Downloaded from https://journals.asm.org/journal/mcb on 24 February 2022 by 2a01:4f9:3b:1ae9::

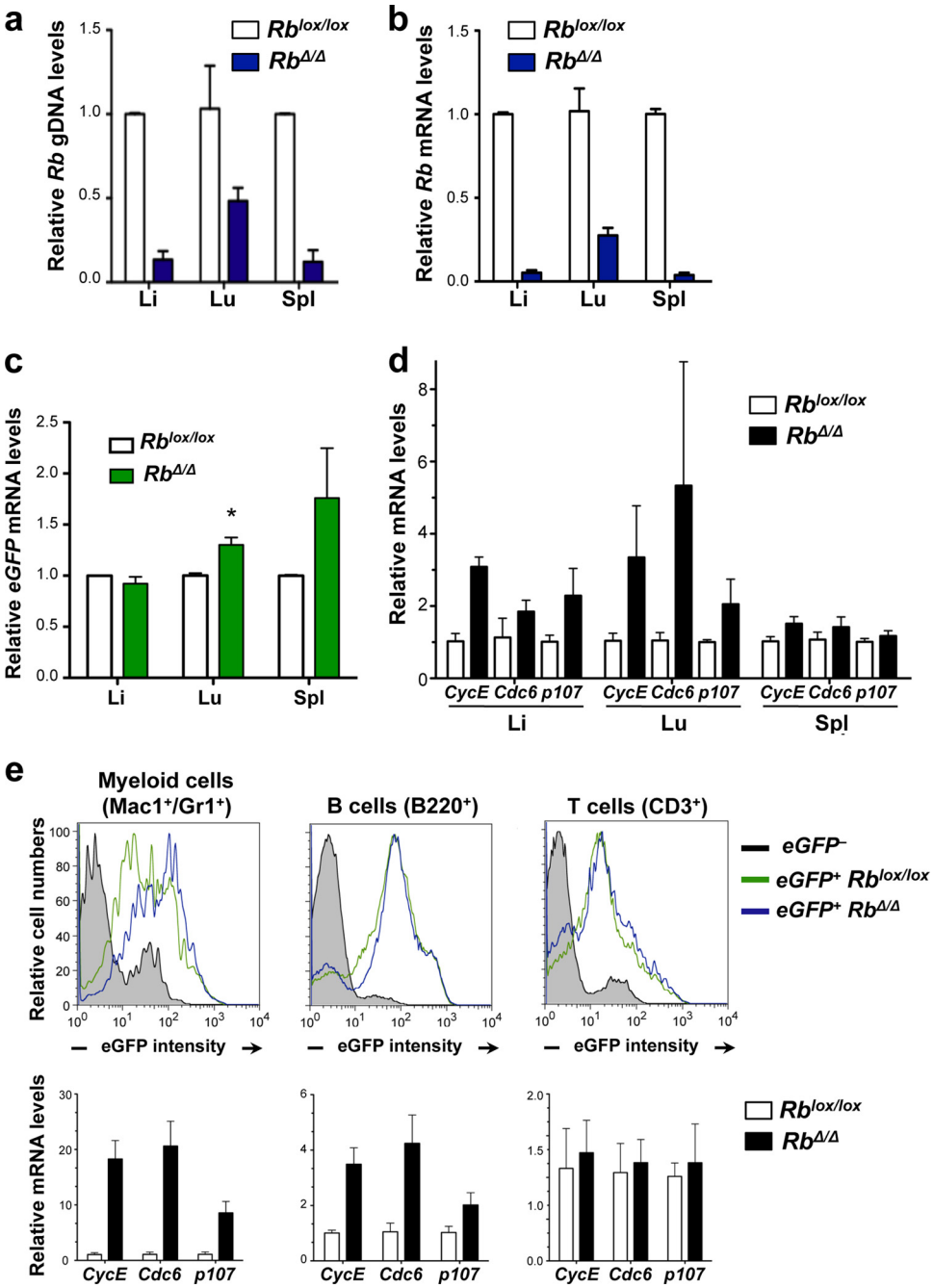

FIG. 8. *RB* negatively regulates its own transcription *in vivo*. (a and b) Analysis by quantitative PCR of deletion of *Rb* in whole organs from adult $Rb^{lox/lox}$; $Rosa26^{CreERT2}$ mice ($Rb^{\Delta/\Delta}$) and $Rb^{lox/lox}$ mice treated with tamoxifen, calculated relative to that for each control organ. Li, liver; Lu, lung; Spl, spleen. (a) qPCR on genomic DNA ($n = 2$) (b) RT-qPCR on mRNA ($n = 3$) (c) Analysis by RT-qPCR of *eGFP* in organs from *Rb-eGFP*; $Rb^{lox/lox}$; $Rosa26^{CreERT2}$ mice ($Rb^{\Delta/\Delta}$) and *Rb-eGFP*; $Rb^{lox/lox}$ ($Rb^{lox/lox}$) mice treated with tamoxifen ($n = 4$). (d) RT-qPCR analysis of *cyclin E* (*CycE*), *Cdc6*, and *p107* in organs from $Rb^{lox/lox}$ and $Rb^{lox/lox}$; $Rosa26^{CreERT2}$ mice treated with tamoxifen ($Rb^{\Delta/\Delta}$) (e) Upper panels: representative ($n = 3$) FACS analysis for eGFP fluorescence in splenic $Mac1^+/Gr1^+$ myeloid cells, $B220^+$ B cells, and $CD3^+$ T cells from control ($eGFP^-$, shaded area), *Rb-eGFP*; $Rb^{lox/lox}$, and *Rb-eGFP*; $Rb^{lox/lox}$; $Rosa26^{CreERT2}$ mice, all treated with tamoxifen. Lower panels: analysis by RT-qPCR of *cyclin E*, *Cdc6*, and *p107* in sorted cells from the spleens of control and *Rb* mutant mice ($n \geq 2$).

days after infection, we found that eGFP levels had decreased in these TKO MEFs (Fig. 10a) to a level similar to that observed in response to deletion of *Rb* alone (Fig. 7b and c), indicating that the decrease in *eGFP* expression observed in response to the deletion of *Rb* only was not due to p107 and/or p130 activity. As suggested earlier, this decrease occurred in spite of the increase in the percentage of cells in S phase and G_2/M phase in TKO MEFs (Fig. 10b), further indicating that the *Rb* promoter is not induced by E2F activity during cell cycle progression.

Downloaded from https://journals.asm.org/journal/mcb on 24 February 2022 by 2a01:4f9:3b:1ae9::

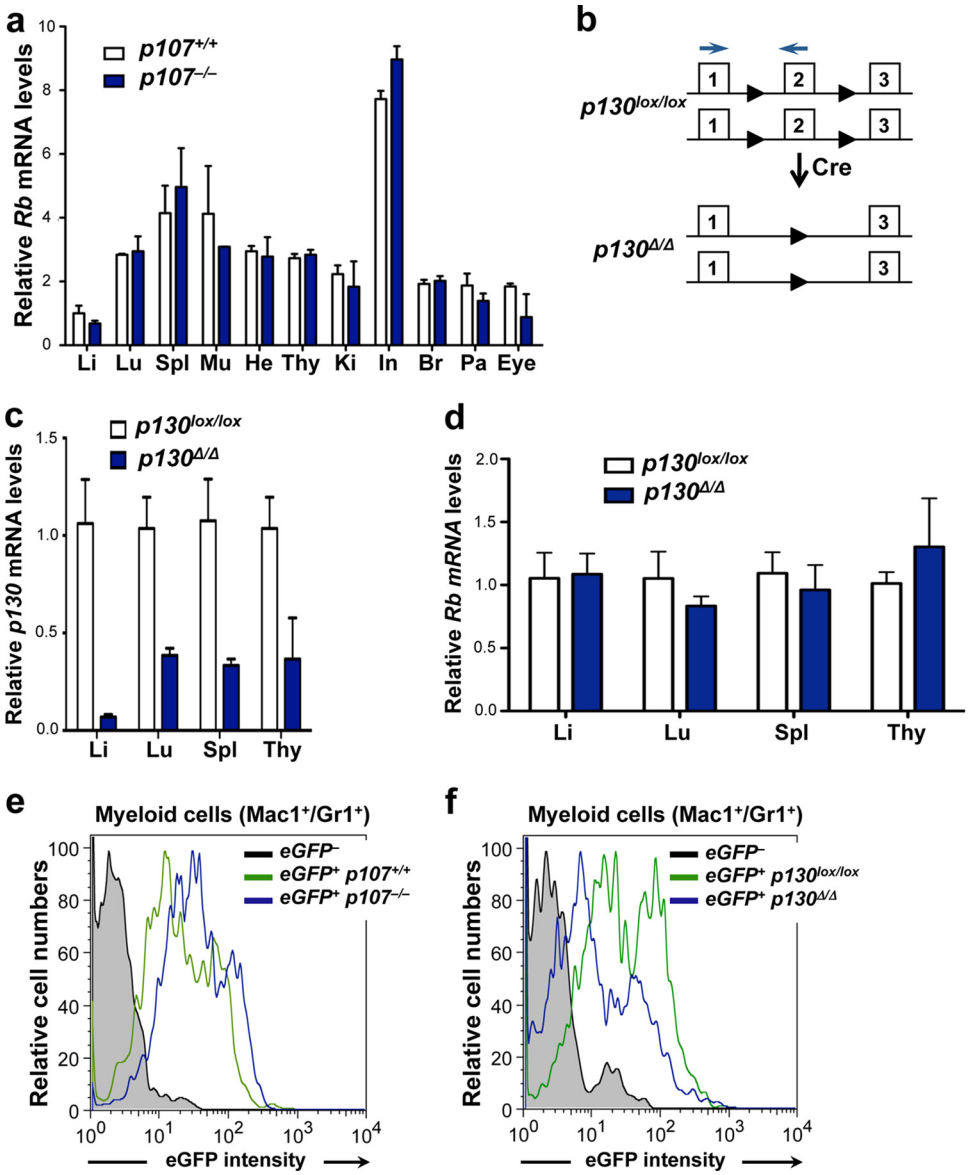

FIG. 9. *p107* and *p130* control of *Rb* transcription *in vivo*. (a) Analysis by RT-qPCR of *Rb* mRNA expression in whole organs from wild-type and *p107*-deficient adult mice relative to the expression of *Rb* in the wild-type liver ($n = 3$). (b) Schematic representation of the conditional $p130^{lox}$ allele. Blue arrows indicate locations of primers used to detect deletion of the *p130* mRNA. Cre-mediated excision results in the genomic deletion of exon 2 and in the loss of *p130* mRNA containing exon 2 sequences. (c) Analysis by RT-qPCR of *p130* in the liver, lung, spleen, and thymus of $p130^{lox/lox}$; $Rosa26^{CreERT2}$ mice and control mice treated with tamoxifen. (d) Analysis by RT-qPCR of *Rb* in the same samples as for panel c. (e) Representative ($n = 3$) FACS analysis for eGFP fluorescence in $Mac1^+/Gr1^+$ splenic cells from control ($eGFP^-$, shaded area), *Rb-eGFP*, and $p107^{-/-}$; *Rb-eGFP* mice. (f) Representative ($n = 2$) FACS analysis for eGFP fluorescence in $Mac1^+/Gr1^+$ splenic cells from control ($eGFP^-$, shaded area), *Rb-eGFP*, and $p130^{lox/lox}$; $Rosa26^{CreERT2}$; *Rb-eGFP* mice. All mice were treated with tamoxifen.

We next determined if loss of *Rb* family genes may have an effect on *Rb* transcription *in vivo*. To this end, we collected control and TKO samples 7 days after the first tamoxifen injection, before the health of the animals was significantly affected (see Materials and Methods). Consistent with our observations with *Rb* mutant mice (Fig. 8a and b), the efficiencies of genomic deletion and reduction in *Rb* mRNA levels were similar in TKO mice (Fig. 10c and data not shown). The efficiencies of genomic deletion and the reduction of *p130* mRNA in TKO mice were similar in the livers and spleens from TKO mice; in the lungs, the reduction in *p130* mRNA levels was more pronounced than the amount of genomic deletion but was still not as strong as in the other organs (Fig. 10c and data not shown). While *eGFP* expression in the liver did not change in any of the single-knockout mice, we found a significant increase in *eGFP* mRNA levels in the liver of TKO mice 1 week after the initial activation of CreER by tamoxifen (Fig. 10d). Similarly, *eGFP* expression increased slightly in the lungs of mice in which *Rb* had been deleted singly, but increased strongly when all three *Rb* family genes were inactivated (Fig. 10d). While not significant, we also observed a trend toward activation of *Rb* transcription in the spleens of

Downloaded from https://journals.asm.org/journal/mcb on 24 February 2022 by 2a01:4f9:3b:1ae9::.

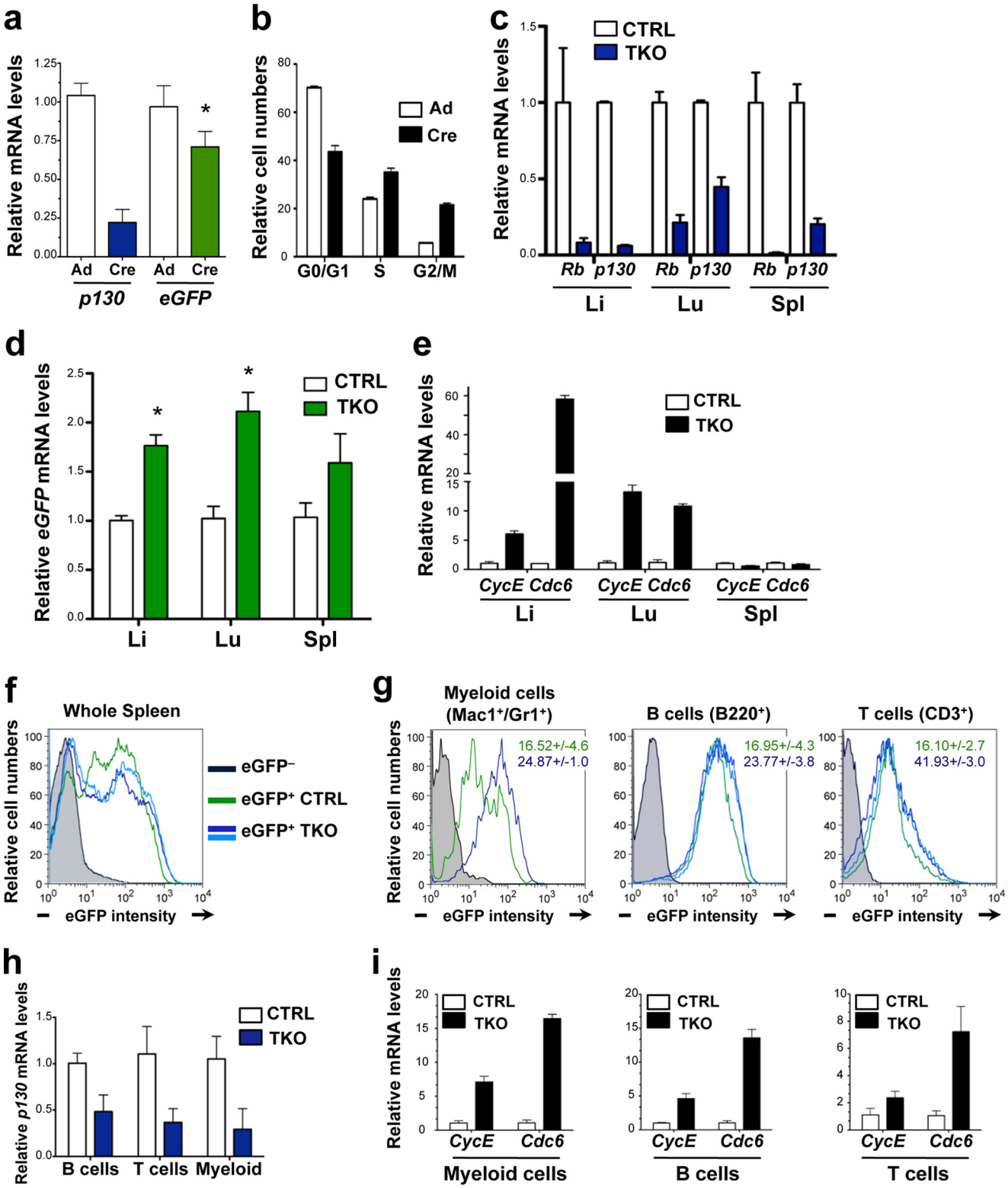

FIG. 10. The RB family regulates the *Rb* promoter *in vivo*. (a) Analysis by RT-qPCR of *p130* and *eGFP* in conditional $Rb^{lox/lox}$; $p130^{lox/lox}$; $p107^{-/-}$ (TKO) MEFs 4 days after infection with Adeno-Cre (Cre) or a control adenovirus (Ad) ($n = 4$). (b) Cell cycle profiles of conditional TKO MEFs infected with Adeno-Cre (Cre) or a control adenovirus (Ad) as for panel a. Percentages were calculated from the results of BrdU/PI FACS analysis ($n = 2$). (c) Analysis by RT-qPCR of *Rb* and *p130* in the livers (Li), lungs (Lu), and spleens (Spl) of conditional $Rosa26^{CreERT2}$ TKO mice (TKO) and control mice (CTRL), all treated with tamoxifen ($n \geq 3$). (d) Analysis by RT-qPCR of *eGFP* in samples similar to those for panel c from *Rb-eGFP* transgenic mice ($n \geq 4$). (e) Analysis by RT-qPCR of *CycE* and *Cdc6* in samples similar to those for panel c ($n \geq 2$). (f) Representative FACS analysis of eGFP expression in control and TKO splenocytes. (g) Representative FACS analysis of eGFP expression in splenic $Mac1^+/Gr1^+$ myeloid cells, $B220^+$ B cells, and $CD3^+$ T cells sorted from control ($eGFP^-$, shaded area), *Rb-eGFP*$^+$, and TKO; *Rb-eGFP*$^+$ mice. Green and blue numbers represent the percentages of $BrdU^+$ cells in control (green) and TKO (blue) populations ($n = 3$). (h) Analysis by RT-qPCR of *p130* in cells isolated as for panel g from control mice and TKO mice. (i) Analysis by RT-qPCR of *CycE* and *Cdc6* from control and TKO mice.

Downloaded from https://journals.asm.org/journal/mcb on 24 February 2022 by 2a01:4f9:3b:1ae9::

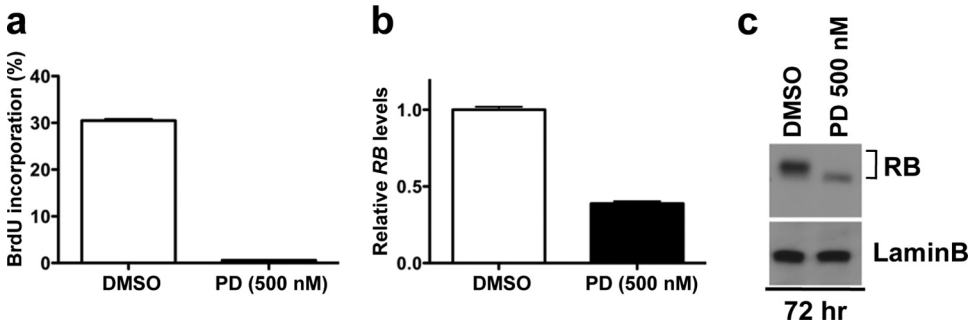

FIG. 11. The RB pathway regulates *RB* expression. (a to c) Analysis of MCF7 cells treated with vehicle (DMSO) or the CDK4 inhibitor PD 033291 (PD). (a) Quantification of BrdU incorporation ($n = 3$). (b) RT-qPCR for *RB* expression relative to that of *GAPDH* ($n = 3$). (c) Western blot analysis of RB and lamin B on protein extracts; bracket indicates hypo- and hyperphosphorylated species of RB.

TKO mice (Fig. 10d). In parallel, we examined the changes in expression of *cyclin E* and *Cdc6* in these TKO organs. We observed that, as in the *Rb* mutant organs, expression of these cell cycle genes increased in both the liver and the lungs of TKO mice, whereas no increase was observed in the whole spleen (Fig. 10e). In comparison to their expression in the *Rb* mutant organs, however, both genes were expressed at much higher levels in the TKO liver and lungs (Fig. 8d and 10e). Furthermore, while these two classical E2F target genes were induced 5- to 60-fold in TKO organs, *eGFP* expression was induced only 1.5- to 2-fold, clearly demonstrating that the *Rb* promoter is controlled by more than just cell cycle-associated activity.

This absence of change in *eGFP* expression could again reflect significant changes in some subpopulations that are masked by less-significant changes (or changes in the other direction) in others. Initial characterization of the spleen showed multiple eGFP peaks, some of which appeared to shift in the TKO mice (Fig. 10f). Within the three main blood cell types in the spleen, only cells of the myeloid lineage ($Mac1^+/Gr1^+$) displayed significantly increased eGFP expression in TKO mice compared to that in the controls, as determined by FACS analysis (Fig. 10g). We verified that Cre was active within these three subpopulations by examining *p130* mRNA levels in TKO and control cells (Fig. 10h). Furthermore, as observed in *Rb* mutant cells, even though RB family mutant B cells and T cells showed increased expression of *CycE* and *Cdc6* and increased incorporation of BrdU (Fig. 10i), these two subpopulations did not show a correlative increase in *eGFP* expression. Thus, the RB family of proteins controls *Rb* transcription in several mouse cell types, *in vivo* and in culture, and this control is not a reflection of changes in cell cycle status.

The RB family is often simultaneously inactivated in human tumors, not through genetic deletion, but rather through mutations in upstream regulators of the pathway, resulting in increased phosphorylation and decreased activity of RB, p107, and p130. To examine the role of the RB pathway in the regulation of *RB* transcription in human cells, we treated human breast cancer cells with PD 033291, a chemical inhibitor of the CDK4 kinase which normally phosphorylates the RB family during G_1. Treatment of cells with this drug was sufficient to block cell cycle progression in MCF7 cancer cells, as measured by BrdU incorporation (Fig. 11a). Inhibition of RB phosphorylation resulted in decreased levels of *RB* mRNA and protein in these cells (Fig. 11b and c). These data further indicate that the RB pathway controls *RB* transcription in human cells.

DISCUSSION

RB is a critical tumor suppressor whose function is inactivated in most, if not all, human cancer cells. While the levels of RB expression may strongly influence the fate of normal and tumor cells, little is known about the mechanisms regulating *RB* mRNA at the transcriptional and posttranscriptional levels. Using a new strain of *Rb-eGFP* BAC reporter mice, we show here that *Rb* mRNA levels are regulated in a tissue-specific manner during embryogenesis and in adult mice. Furthermore, these observations suggest that *Rb* transcription is controlled by distal elements and/or posttranscriptional mechanisms in mice. Finally, we show for the first time that members of the RB family bind directly to and regulate the *RB* promoter in both mice and humans, identifying novel regulatory feedback loops within the RB pathway in mammalian cells.

Control of *RB* expression at the transcriptional and posttranscriptional levels. *Rb-eGFP* BAC reporter mice reveal that dynamic transcriptional control of *Rb* occurs in embryonic and adult cells in mouse organs and tissues. For instance, we found that *Rb* expression is controlled at the transcriptional level in specific cell populations, including myeloid cells and the retinas of adult mice. In the future, the development of strategies to increase *RB* transcription in human cells may lead to increased RB protein levels and may block the proliferation of tumor cells with mutations in upstream regulators of RB, for example, by saturating the kinase activities of cyclin/Cdk complexes.

Previous transgenic reporter systems failed to recapitulate *Rb* transcription in liver and muscle cells of mouse embryos (1, 25). The longer regulatory regions present in the *Rb-eGFP* BAC provide enough information to drive the expression of the reporter gene in heart and skeletal muscle cells in transgenic embryos. Thus, the elements controlling *Rb* expression in muscle cells lie outside of the proximal promoter region. RB is a critical mediator of muscle differentiation (12), and it will be interesting in future experiments to generate additional reporter strains to further localize these regulatory elements. Furthermore, *Rb* has been described to be regulated directly by another critical tumor suppressor, p53 (34), and this regulation has been shown to be important for myogenesis in culture (37).

Downloaded from https://journals.asm.org/journal/mcb on 24 February 2022 by 2a01:4f9:3b:1ae9::

Rb-eGFP BAC reporter mice could be used to identify the functional importance of the p53/RB transcriptional connection in muscle cells and during tumor development.

Even the BAC transgenic reporter fails to fully recapitulate *Rb* expression in some tissues, both in embryos and in adult mice. While this limits the potential use of *Rb-eGFP* BAC reporter mice to study the mechanisms controlling *Rb* transcription in these organs, these observations also raise interesting questions. For instance, the *eGFP* reporter is not expressed in the liver of transgenic embryos, where *Rb* is normally strongly expressed. We first investigated the possibility that the high levels of *Rb* in the embryonic liver could be due to an alternative transcription start site downstream of the *eGFP* insertion in exon 1. However, through RT-qPCR analysis, we observed that the endogenous *Rb* liver transcripts include sequences of exon 1 that are upstream of the *eGFP* insertion site, ruling out this possibility in the embryonic liver (data not shown). Therefore, we believe that the differing expression levels observed in the embryonic liver, as well as the adult thymus and kidney, are likely due to a difference in the regulation of the *Rb* and *eGFP* transcripts. One possible mechanism through which regulation of *eGFP* could be different from that of *Rb* could be the absence of a distant enhancer element in our transgene. A second possibility could be that, despite the length of the BAC, the chromatin structure of the *Rb-eGFP* transgene is different from that of the endogenous *Rb* allele in particular cell types. Finally, the *Rb* mRNA may be subject to posttranscriptional regulation that does not affect the *eGFP* mRNA, or the *eGFP* mRNA could be more stable than the *Rb* mRNA. We believe that a differential regulation of the *Rb* mRNA is more likely, because we recently described the use of a similar BAC transgenic reporter for the *Rb* family member *p107* and did not observe any unusual stability or instability of the RNA from the same *eGFP* cassette in the liver or other organs (except the testes) of these transgenic mice (8). Posttranscriptional regulation of *Rb* may explain why *eGFP* is expressed at higher levels in the adult kidney than is *Rb*, as the *eGFP* transcript is missing any 3′ UTR sequences that could be regulated by endogenous microRNAs. Recently miR-106 has been described to potentially downregulate *RB* expression in human tumor samples (21), underscoring the importance of understanding the role of posttranscriptional regulation of *RB* in normal cells and cancer cells.

Positive and negative regulation of RB transcription by RB family members. It is particularly interesting to note that while *eGFP* expression generally increases *in vivo* in response to the loss of *Rb* or the entire *Rb* gene family in *Rb-eGFP* transgenic mice, in MEFs *eGFP* expression actually decreases when *Rb* family function is deleted. This observation suggests that RB, and potentially p107 and p130, may positively regulate the *Rb* promoter in this specific cellular context. Although we cannot exclude that the decrease in *Rb* promoter activity is the result of indirect effects of the loss of RB, these results suggest that RB may be able to both positively and negatively regulate its own promoter, depending on the context, a finding that is consistent with the conflicting observations in the literature (see the introduction). While the loss of RB alone increased *eGFP* levels in the spleen and the loss of p130 alone slightly decreased *Rb* and *eGFP* levels in the spleen, the triple-knockout mice showed no significant changes in *eGFP* expression in this organ. This result suggests that RB and p130 may have opposing roles at the *Rb* promoter in splenic cells. Alternatively, the variation in the effects of the RB family on *Rb-eGFP* expression may reflect more-distinct changes within splenic subpopulations. In both cases, these observations underscore the complexity of *Rb* regulation and its dynamism *in vivo*.

We also observed that expression of *Rb* and the *Rb-eGFP* transgene frequently increased in quiescent MEFs upon knockdown of either *p107* or *p130* (data not shown). However, this observation is variable, suggesting that RB family members together regulate the *Rb* promoter without a clearly defined requirement for any individual member. This result is consistent with the observation *in vivo* that only subtle effects on *Rb* expression are observed in the absence of a single *Rb* family member, whereas stronger effects are observed in the absence of the entire family. Future experiments will include comparing the effects of deleting combinations of two *Rb* family genes to ascertain the role of each RB family member in the control of *Rb* transcription.

RB transcription during cell cycle progression. Because the *RB* promoter contains an E2F binding site, an attractive hypothesis was that *RB* expression is increased during cell cycle progression, which may serve as a negative feedback mechanism to control cell proliferation. One argument in favor of this idea was that *Rb* levels are high early during embryogenesis when many cells divide and become lower as embryos mature (25). A second argument is the more-pronounced changes in *Rb* transcription observed in TKO cells, which often cycle more than single-knockout and wild-type cells. However, in wild-type animals, cycling organs like the thymus and spleen do not express significantly more *Rb* or *Rb-eGFP* mRNA than the heart or muscle, which are largely noncycling. In addition, in many instances, we found no correlation between *Rb* mRNA levels, the expression of canonical E2F target genes, and the cell cycle status of the cells. Furthermore, we even observed lower levels of *Rb* transcription (as measured by the *eGFP* reporter) in *Rb* mutant and TKO MEFs compared to levels in control MEFs. This does not exclude that *Rb* transcription is cell cycle regulated, as we observed in cell cycle reentry experiments in MEFs. Together, these observations suggest a complex model of *Rb* transcriptional regulation in which a combination of tissue-specific and general transcription factors, including E2F, ATF, and Sp1, together control *Rb* transcription. Whether all or some of these factors are under the control of RB family members is still under investigation.

Functional compensation within the *RB* gene family and *RB* autoregulation. One model to explain the specificity of tumor development in *RB* patients and *Rb* mutant mice is that loss of RB results in a cell-type-specific compensatory upregulation of *p107* transcription (16 and references therein). Thus, the fact that *p107*- and *p130*-deficient mice are not cancer prone (28, 29) may be due to compensation by the other two RB family members, especially RB. Based on this model, we speculated that increased transcription of *Rb* in either $p107^{-/-}$ or $p130^{-/-}$ mice could contribute to the compensatory functions of RB. We did observe that this feedback loop occurs in specific cell types, suggesting that transcriptional upregulation of *RB* in *p107* or *p130* mutant cells may provide tumor-suppressive feedback.

What could be the role of *RB* autoregulation? In the cells of

Downloaded from https://journals.asm.org/journal/mcb on 24 February 2022 by 2a01:4f9:3b:1ae9::

patients who inherit one defective allele of *RB*, half the amount of RB should be made. If RB positively regulates its own promoter, this feedback mechanism could lead to even lower levels of RB; if RB negatively regulates its own transcription, then compensatory levels of RB may be produced. Evidence for this autoregulation of RB in patients has already been observed (17). Using *Rb-eGFP* transgenic mice, we found that RB may mostly repress its own transcription, suggesting that cells have evolved a mechanism to compensate for the loss of one *RB* allele. However, *Rb*-deficient mouse pituitary tumor cells did not display derepression of a *lacZ* reporter for *Rb* transcription, suggesting that RB does not autoregulate itself in this context, again emphasizing that regulation of *Rb* by its own protein product may be highly cell type specific (1). Loss of the function of $p16^{INK4a}$ or activating mutations in CDK4, both commonly found in human cancers (7), lead to increased RB phosphorylation and inhibit RB cellular functions; this in turn may result in increased *RB* transcription in a compensatory feedback mechanism, as is suggested by analysis of human bladder cancers (3). Future experiments will continue to dissect the mechanisms controlling *RB* transcription in various types of normal and cancer cells.

ACKNOWLEDGMENTS

We are grateful to David MacPherson for his critical reading of the manuscript and the members of the Sage lab for helpful discussions throughout this work. We also thank Pauline Chu for her help with histology.

This work was supported by National Cancer Institute grant 5R01CA114102 and by the Damon Runyon Cancer Research Foundation (to J. Sage). D. L. Burkhart received a California Breast Cancer Research Program dissertation fellowship and P. Viatour a Human Frontier Science Program postdoctoral fellowship.

There are no potential conflicts of interest to disclose.

REFERENCES

1. **Agromayor, M., E. Wloga, B. Naglieri, J. Abrashkin, K. Verma, and L. Yamasaki.** 2006. Visualizing dynamic E2F-mediated repression in vivo. Mol. Cell. Biol. **26:**4448–4461.
2. **Balciunaite, E., A. Spektor, N. H. Lents, H. Cam, H. Te Riele, A. Scime, M. A. Rudnicki, R. Young, and B. D. Dynlacht.** 2005. Pocket protein complexes are recruited to distinct targets in quiescent and proliferating cells. Mol. Cell. Biol. **25:**8166–8178.
3. **Benedict, W. F., S. P. Lerner, J. Zhou, X. Shen, H. Tokunaga, and B. Czerniak.** 1999. Level of retinoblastoma protein expression correlates with p16 (MTS-1/INK4A/CDKN2) status in bladder cancer. Oncogene **18:**1197–1203.
4. **Bookstein, R., P. Rio, S. A. Madreperla, F. Hong, C. Allred, W. E. Grizzle, and W. H. Lee.** 1990. Promoter deletion and loss of retinoblastoma gene expression in human prostate carcinoma. Proc. Natl. Acad. Sci. U. S. A. **87:**7762–7766.
5. **Botos, J., R. Smith III, and D. T. Kochevar.** 2002. Retinoblastoma function is a better indicator of cellular phenotype in cultured breast adenocarcinoma cells than retinoblastoma expression. Exp. Biol. Med. (Maywood) **227:**354–362.
6. **Braden, W. A., A. K. McClendon, and E. S. Knudsen.** 2008. Cyclin-dependent kinase 4/6 activity is a critical determinant of pre-replication complex assembly. Oncogene **27:**7083–7093.
7. **Burkhart, D. L., and J. Sage.** 2008. Cellular mechanisms of tumour suppression by the retinoblastoma gene. Nat. Rev. Cancer. **8:**671–682.
8. **Burkhart, D. L., P. Viatour, V. M. Ho, and J. Sage.** 2008. GFP reporter mice for the retinoblastoma-related cell cycle regulator p107. Cell Cycle **7:**2544–2552.
9. **Chen, H. Z., S. Y. Tsai, and G. Leone.** 2009. Emerging roles of E2Fs in cancer: an exit from cell cycle control. Nat. Rev. Cancer **9:**785–797.
10. **Classon, M., and N. Dyson.** 2001. p107 and p130: versatile proteins with interesting pockets. Exp. Cell Res. **264:**135–147.
11. **Cordon-Cardo, C., and V. M. Richon.** 1994. Expression of the retinoblastoma protein is regulated in normal human tissues. Am. J. Pathol. **144:**500–510.
12. **De Falco, G., F. Comes, and C. Simone.** 2006. pRb: master of differentiation. Coupling irreversible cell cycle withdrawal with induction of muscle-specific transcription. Oncogene **25:**5244–5249.
13. **DeGregori, J., T. Kowalik, and J. R. Nevins.** 1995. Cellular targets for activation by the E2F1 transcription factor include DNA synthesis- and G1/S-regulatory genes. Mol. Cell. Biol. **15:**4215–4224.
14. **Deléhouzée, S., T. Yoshikawa, C. Sawa, J. Sawada, T. Ito, M. Omori, T. Wada, Y. Yamaguchi, Y. Kabe, and H. Handa.** 2005. GABP, HCF-1 and YY1 are involved in Rb gene expression during myogenesis. Genes Cells **10:**717–731.
15. **Di Fiore, B., A. Palena, A. Felsani, F. Palitti, M. Caruso, and P. Lavia.** 1999. Cytosine methylation transforms an E2F site in the retinoblastoma gene promoter into a binding site for the general repressor methylcytosine-binding protein 2 (MeCP2). Nucleic Acids Res. **27:**2852–2859.
16. **Donovan, S. L., B. Schweers, R. Martins, D. Johnson, and M. A. Dyer.** 2006. Compensation by tumor suppressor genes during retinal development in mice and humans. BMC Biol. **4:**14.
17. **Dunn, J. M., R. A. Phillips, X. Zhu, A. Becker, and B. L. Gallie.** 1989. Mutations in the RB1 gene and their effects on transcription. Mol. Cell. Biol. **9:**4596–4604.
18. **Fujita, T., N. Ohtani-Fujita, and T. Sakai.** 1996. Identification of an RB-responsive region in the 5′ untranslated region of the RB gene. Cancer Lett. **101:**149–157.
19. **Gill, R. M., P. A. Hamel, J. Zhe, E. Zacksenhaus, B. L. Gallie, and R. A. Phillips.** 1994. Characterization of the human RB1 promoter and of elements involved in transcriptional regulation. Cell Growth Differ. **5:**467–474.
20. **Gope, M. L., M. Chun, and R. Gope.** 1991. Comparative study of the expression of Rb and p53 genes in human colorectal cancers, colon carcinoma cell lines and synchronized human fibroblasts. Mol. Cell. Biochem. **107:**55–63.
21. **Guo, J., Y. Miao, B. Xiao, R. Huan, Z. Jiang, D. Meng, and Y. Wang.** 2009. Differential expression of microRNA species in human gastric cancer versus non-tumorous tissues. J. Gastroenterol. Hepatol. **24:**652–657.
22. **Hamel, P. A., R. M. Gill, R. A. Phillips, and B. L. Gallie.** 1992. Transcriptional repression of the E2-containing promoters EIIaE, c-myc, and RB1 by the product of the RB1 gene. Mol. Cell. Biol. **12:**3431–3438.
23. **Hateboer, G., A. Wobst, B. O. Petersen, L. Le Cam, E. Vigo, C. Sardet, and K. Helin.** 1998. Cell cycle-regulated expression of mammalian CDC6 is dependent on E2F. Mol. Cell. Biol. **18:**6679–6697.
24. **Jiang, Z., Z. Guo, F. A. Saad, J. Ellis, and E. Zacksenhaus.** 2001. Retinoblastoma gene promoter directs transgene expression exclusively to the nervous system. J. Biol. Chem. **276:**593–600.
25. **Jiang, Z., E. Zacksenhaus, B. L. Gallie, and R. A. Phillips.** 1997. The retinoblastoma gene family is differentially expressed during embryogenesis. Oncogene **14:**1789–1797.
26. **Kim, S. J., U. S. Onwuta, Y. I. Lee, R. Li, M. R. Botchan, and P. D. Robbins.** 1992. The retinoblastoma gene product regulates Sp1-mediated transcription. Mol. Cell. Biol. **12:**2455–2463.
27. **Kim, S. J., S. Wagner, F. Liu, M. A. O'Reilly, P. D. Robbins, and M. R. Green.** 1992. Retinoblastoma gene product activates expression of the human TGF-beta 2 gene through transcription factor ATF-2. Nature **358:**331–334.
28. **LeCouter, J. E., B. Kablar, W. R. Hardy, C. Ying, L. A. Megeney, L. L. May, and M. A. Rudnicki.** 1998. Strain-dependent myeloid hyperplasia, growth deficiency, and accelerated cell cycle in mice lacking the Rb-related p107 gene. Mol. Cell. Biol. **18:**7455–7465.
29. **LeCouter, J. E., B. Kablar, P. F. Whyte, C. Ying, and M. A. Rudnicki.** 1998. Strain-dependent embryonic lethality in mice lacking the retinoblastoma-related p130 gene. Development **125:**4669–4679.
30. **Matsumoto, T., N. Ohtani-Fujita, Y. Sowa, F. Bai, T. Nikaido, T. Tamaki, and T. Sakai.** 1998. Cell cycle-dependent modulation of promoter activities of RB and WAF1/Cip1 genes. Jpn. J. Cancer Res. **89:**626–633.
31. **Mercader, J., J. Ribot, I. Murano, S. Feddersen, S. Cinti, L. Madsen, K. Kristiansen, M. L. Bonet, and A. Palou.** 2009. Haploinsufficiency of the retinoblastoma protein gene reduces diet-induced obesity, insulin resistance, and hepatosteatosis in mice. Am. J. Physiol. Endocrinol. Metab. **297:**E184–E193.
32. **Nikitin, A., B. Shan, A. Flesken-Nikitin, K. H. Chang, and W. H. Lee.** 2001. The retinoblastoma gene regulates somatic growth during mouse development. Cancer Res. **61:**3110–3118.
33. **Ohtani-Fujita, N., T. Fujita, R. Takahashi, P. D. Robbins, T. P. Dryja, and T. Sakai.** 1994. A silencer element in the retinoblastoma tumor-suppressor gene. Oncogene **9:**1703–1711.
34. **Osifchin, N. E., D. Jiang, N. Ohtani-Fujita, T. Fujita, M. Carroza, S. J. Kim, T. Sakai, and P. D. Robbins.** 1994. Identification of a p53 binding site in the human retinoblastoma susceptibility gene promoter. J. Biol. Chem. **269:**6383–6389.
35. **Park, K., J. Choe, N. E. Osifchin, D. J. Templeton, P. D. Robbins, and S. J. Kim.** 1994. The human retinoblastoma susceptibility gene promoter is positively autoregulated by its own product. J. Biol. Chem. **269:**6083–6088.
36. **Passegué, E., A. J. Wagers, S. Giuriato, W. C. Anderson, and I. L. Weissman.** 2005. Global analysis of proliferation and cell cycle gene expression in the

Downloaded from https://journals.asm.org/journal/mcb on 24 February 2022 by 2a01:4f9:3b:1ae9::

regulation of hematopoietic stem and progenitor cell fates. J. Exp. Med. **202:**1599–1611.

37. **Porrello, A., M. A. Cerone, S. Coen, A. Gurtner, G. Fontemaggi, L. Cimino, G. Piaggio, A. Sacchi, and S. Soddu.** 2000. p53 regulates myogenesis by triggering the differentiation activity of pRb. J. Cell Biol. **151:**1295–1304.
38. **Roesch, A., B. Becker, S. Meyer, C. Hafner, P. J. Wild, M. Landthaler, and T. Vogt.** 2005. Overexpression and hyperphosphorylation of retinoblastoma protein in the progression of malignant melanoma. Mod. Pathol. **18:**565–572.
39. **Sage, J., A. L. Miller, P. A. Perez-Mancera, J. M. Wysocki, and T. Jacks.** 2003. Acute mutation of retinoblastoma gene function is sufficient for cell cycle re-entry. Nature **424:**223–228.
40. **Sage, J., G. J. Mulligan, L. D. Attardi, A. Miller, S. Chen, B. Williams, E. Theodorou, and T. Jacks.** 2000. Targeted disruption of the three Rb-related genes leads to loss of G(1) control and immortalization. Genes Dev. **14:** 3037–3050.
41. **Sakai, T., N. Ohtani, T. L. McGee, P. D. Robbins, and T. P. Dryja.** 1991. Oncogenic germ-line mutations in Sp1 and ATF sites in the human retinoblastoma gene. Nature **353:**83–86.
42. **Sankaran, V. G., S. H. Orkin, and C. R. Walkley.** 2008. Rb intrinsically promotes erythropoiesis by coupling cell cycle exit with mitochondrial biogenesis. Genes Dev. **22:**463–475.
43. **Shan, B., C. Y. Chang, D. Jones, and W. H. Lee.** 1994. The transcription factor E2F-1 mediates the autoregulation of RB gene expression. Mol. Cell. Biol. **14:**299–309.
44. **Sherr, C. J., and F. McCormick.** 2002. The RB and p53 pathways in cancer. Cancer Cell **2:**103–112.
45. **Spencer, C., S. Pajovic, H. Devlin, Q. D. Dinh, T. W. Corson, and B. L. Gallie.** 2005. Distinct patterns of expression of the RB gene family in mouse and human retina. Gene Expr. Patterns **5:**687–694.
46. **Spike, B. T., A. Dirlam, B. C. Dibling, J. Marvin, B. O. Williams, T. Jacks, and K. F. Macleod.** 2004. The Rb tumor suppressor is required for stress erythropoiesis. EMBO J. **23:**4319–4329.
47. **Stengel, K. R., C. Thangavel, D. A. Solomon, S. P. Angus, Y. Zheng, and E. S. Knudsen.** 2009. Retinoblastoma/p107/p130 pocket proteins: protein dynamics and interactions with target gene promoters. J. Biol. Chem. **284:**19265–19271.
48. **Takahashi, Y., J. Rayman, and B. Dynlacht.** 2000. Analysis of promoter binding by the E2F and pRB families in vivo: distinct E2F proteins mediate activation and repression. Genes Dev. **14:**804–816.
49. **Trimarchi, J. M., and J. A. Lees.** 2002. Sibling rivalry in the E2F family. Nat. Rev. Mol. Cell Biol. **3:**11–20.
50. **Vandromme, M., C. Chailleux, F. Escaffit, and D. Trouche.** 2008. Binding of the retinoblastoma protein is not the determinant for stable repression of some E2F-regulated promoters in muscle cells. Mol. Cancer Res. **6:**418–425.
51. **Ventura, A., D. G. Kirsch, M. E. McLaughlin, D. A. Tuveson, J. Grimm, L. Lintault, J. Newman, E. E. Reczek, R. Weissleder, and T. Jacks.** 2007. Restoration of p53 function leads to tumour regression in vivo. Nature **445:**661–665.
52. **Viatour, P., T. C. Somervaille, S. Venkatasubrahmanyam, S. Kogan, M. E. McLaughlin, I. L. Weissman, A. J. Butte, E. Passegue, and J. Sage.** 2008. Hematopoietic stem cell quiescence is maintained by compound contributions of the retinoblastoma gene family. Cell Stem Cell **3:**416–428.
53. **Walkley, C. R., and S. H. Orkin.** 2006. Rb is dispensable for self-renewal and multilineage differentiation of adult hematopoietic stem cells. Proc. Natl. Acad. Sci. U. S. A. **103:**9057–9062.
54. **Walkley, C. R., J. M. Shea, N. A. Sims, L. E. Purton, and S. H. Orkin.** 2007. Rb regulates interactions between hematopoietic stem cells and their bone marrow microenvironment. Cell **129:**1081–1095.
55. **Weinberg, R. A.** 1995. The retinoblastoma protein and cell cycle control. Cell **81:**323–330.
56. **Wells, J., and P. J. Farnham.** 2002. Characterizing transcription factor binding sites using formaldehyde crosslinking and immunoprecipitation. Methods **26:**48–56.
57. **Zheng, L., A. Flesken-Nikitin, P. L. Chen, and W. H. Lee.** 2002. Deficiency of retinoblastoma gene in mouse embryonic stem cells leads to genetic instability. Cancer Res. **62:**2498–2502.
58. **Zhu, L., E. Xie, and L. S. Chang.** 1995. Differential roles of two tandem E2F sites in repression of the human p107 promoter by retinoblastoma and p107 proteins. Mol. Cell. Biol. **15:**3552–3562.

Downloaded from https://journals.asm.org/journal/mcb on 24 February 2022 by 2a01:4f9:3b:1ae9::